

# H-MIMO - A Hybrid of Spatial Multiplexing and Adaptive Beamforming

by

GuBong Lim

A thesis submitted to the Faculty of the University of Delaware in partial fulfillment of the requirements for the degree of Master of Electrical Engineering

Summer 2005

© 2005 GuBong Lim  
All Rights Reserved

UMI Number: 1428176



UMI Microform 1428176

Copyright 2005 by ProQuest Information and Learning Company.  
All rights reserved. This microform edition is protected against  
unauthorized copying under Title 17, United States Code.

---

ProQuest Information and Learning Company  
300 North Zeeb Road  
P.O. Box 1346  
Ann Arbor, MI 48106-1346

# H-MIMO - A Hybrid of Spatial Multiplexing and Adaptive Beamforming

by

GuBong Lim

Approved: \_\_\_\_\_

Leonard J. Cimini, Jr., Ph.D.

Professor in charge of thesis on behalf of the Advisory Committee

Approved: \_\_\_\_\_

Gonzalo R. Arce, Ph.D.

Chair of the Department of Electrical and Computer Engineering

Approved: \_\_\_\_\_

Eric W. Kaler, Ph.D.

Dean of College of Engineering of the University of Delaware

Approved: \_\_\_\_\_

Conrado M. Gempesaw II, Ph.D.

Vice Provost for Academic and International Programs

## ACKNOWLEDGMENTS

First and foremost, I would like to express my extreme gratitude to my advisor, Dr. Leonard J. Cimini, Jr., for his invaluable insight and comments. I would have to admit that I feel the utmost happiness with his expertise of the field. I also would like to thank to him for his invaluable support, considerate guidance, and endless encouragement as a personal mentor which will extend into my whole life.

I am very grateful to Dr. Larry J. Greenstein who has provided precious technical comments, suggestions, and fruitful discussion during the course of this research. I also wish to thank Dr. Severine Catreux-Erceg for her generous technical support that strongly contributed to this work.

I would like to give special thanks to the Korean government for funding me during my graduate studies, which has given me a priceless chance to be standing at this very momentous point of my life.

I would like to express my thanks to the group of friends whom I am indebted to for their sincere encouragement and help: dear Ilryeol Kim, Seungryong Lee, Joonwoo Choi, Jonghyun Kim, and Erdem Bala.

And finally...

I would like to thank my parents, JongKyu Lim and OakJin Ha, and my older and younger sisters for their unconditional love and immeasurable supports. I could not have finished my degree without them. I dedicate my thesis to my whole family.

# TABLE OF CONTENTS

<b>LIST OF FIGURES</b> . . . . .	<b>vii</b>
----------------------------------	------------

## Chapter

<b>1 INTRODUCTION</b> . . . . .	<b>1</b>
1.1 Motivation . . . . .	1
1.2 Objective and Contributions . . . . .	2
1.3 Outline of the Thesis . . . . .	3
1.4 List of Acronyms . . . . .	3
<b>2 THE RADIO CHANNEL</b> . . . . .	<b>5</b>
2.1 Path Loss . . . . .	5
2.2 Shadow Fading . . . . .	6
2.3 Multipath Fading . . . . .	6
2.4 Delay Spread . . . . .	9
2.5 Doppler Spread . . . . .	10
<b>3 MULTIPLE ANTENNA SYSTEMS</b> . . . . .	<b>11</b>
3.1 Multiple Antenna Techniques . . . . .	11
3.1.1 Spatial Diversity . . . . .	11
3.1.2 Adaptive Beamforming . . . . .	12
3.1.3 Spatial Multiplexing . . . . .	13
3.2 Multiple Antenna Information Theory . . . . .	14
3.3 Criteria for Optimal Weight Vectors . . . . .	18
3.3.1 Minimum Mean Square Error (MMSE) Criterion . . . . .	18

3.3.2	Maximum Signal-to-Interference-plus-Noise-Ratio (MSINR) Criterion . . . . .	20
<b>4</b>	<b>LINK AND CHANNEL MODELS . . . . .</b>	<b>22</b>
4.1	Link Model for H-MIMO with Transmitter (Tx) Beamforming . . . . .	22
4.2	Link Model for H-MIMO without Tx Beamforming . . . . .	24
4.3	Channel Model . . . . .	26
<b>5</b>	<b>SYSTEM MODEL AND RECEIVER PROCESSING . . . . .</b>	<b>28</b>
5.1	Cochannel Interference Condition . . . . .	28
5.2	Receiver Processing for Multiple Antenna Systems . . . . .	29
5.2.1	Receiver Weighting for H-MIMO with Tx Beamforming . . . . .	30
5.2.2	Receiver Weighting for H-MIMO without Tx Beamforming . . . . .	31
<b>6</b>	<b>SIMULATION RESULTS AND DISCUSSION . . . . .</b>	<b>33</b>
6.1	Capacity Evaluation . . . . .	33
6.2	Capacity Versus Distance for CCI #1 . . . . .	34
6.2.1	The impact of Ricean K factor . . . . .	36
6.2.2	The impact of reuse factor . . . . .	36
6.2.3	The impact of target outage probability . . . . .	38
6.3	Capacity Distribution for CCI #1 . . . . .	38
6.3.1	The impact of Ricean K factor . . . . .	39
6.3.2	The impact of reuse factor . . . . .	40
6.3.3	The impact of median SNR . . . . .	41
6.3.4	The impact of the number of cochannel interferers . . . . .	42
6.4	Capacity Versus Distance for CCI #2 . . . . .	43
6.5	Capacity Distribution for CCI #2 . . . . .	45
6.6	Mean Spectral Efficiency . . . . .	45
6.7	No Transmitter Beamforming . . . . .	47
6.8	Capacity Distribution for an 8x8 System . . . . .	47
6.9	Capacity Distribution for a 4x8 System . . . . .	52
<b>7</b>	<b>CONCLUSIONS AND FUTURE WORK . . . . .</b>	<b>54</b>

## LIST OF FIGURES

<b>2.1</b>	Radio environment . . . . .	8
<b>3.1</b>	1x4 diversity system . . . . .	12
<b>3.2</b>	4x4 beamforming system . . . . .	13
<b>3.3</b>	4x4 spatial multiplexing system . . . . .	14
<b>3.4</b>	1x4 SIMO system . . . . .	15
<b>3.5</b>	4x1 MISO system . . . . .	16
<b>3.6</b>	4x4 MIMO system . . . . .	17
<b>4.1</b>	Hybrid system configurations for hybrid IS2 (upper) and hybrid IS3 (lower) . . . . .	23
<b>6.1</b>	Outage capacity versus distance for CCI #1 for a reuse factor of 7 and outage=10% (a) K=0 (b) K=10 . . . . .	34
<b>6.2</b>	Outage capacity versus distance for CCI #1 for a reuse factor of 1 and outage=10% (a) K=0 (b) K=10 . . . . .	35
<b>6.3</b>	Outage capacity versus distance for CCI #1 for a reuse factor of 7, outage=1%, and K=10 . . . . .	37
<b>6.4</b>	CCDF of the capacity for CCI #1 for a reuse factor of 7 (a) K=0 (b) K=10 . . . . .	38
<b>6.5</b>	CCDF of the capacity for CCI #1 for a reuse factor of 1 (a) K=0 (b) K=10 . . . . .	39
<b>6.6</b>	CCDF of the capacity for CCI #1 for a reuse factor of 7 and K=50	40

<b>6.7</b>	90% and 50% (median) capacity as a function of Ricean K factor . .	41
<b>6.8</b>	90% capacity as a function of median SNR at the cell boundary for a reuse factor of 7 (a) K=0 (b) K=10 . . . . .	42
<b>6.9</b>	CCDF of the capacity for CCI #1 when cochannel base stations transmit only one substream for a reuse factor of 7 and K=10 . . .	43
<b>6.10</b>	Outage capacity versus distance for CCI #2 (a) K=0, Reuse=7, (b) K=10, Reuse=7, (C) K=0, Reuse=1, (d) K=10, Reuse=1 . . . . .	44
<b>6.11</b>	CCDF of the capacity for CCI #2 (a) K=0, Reuse=7, (b) K=10, Reuse=7, (C) K=0, Reuse=1, (d) K=10, Reuse=1 . . . . .	46
<b>6.12</b>	CCDF of the capacity with no transmitter beamforming (a) K=0, Reuse=7, (b) K=10, Reuse=7, (C) K=0, Reuse=1, (d) K=10, Reuse=1 . . . . .	48
<b>6.13</b>	CCDF of the capacity for an 8x8 system for a reuse factor of 7 (a) K=0 (b) K=10 . . . . .	49
<b>6.14</b>	CCDF of the capacity for an 8x8 system for a reuse factor of 7 and K=50 . . . . .	50
<b>6.15</b>	CCDF of the capacity when cochannel base stations transmit only one substream for a reuse factor of 7 (a) K=0 (b) K=10 . . . . .	50
<b>6.16</b>	CCDF of the capacity with no transmitter beamforming for a reuse factor of 7 (a) K=0 (b) K=10 . . . . .	51
<b>6.17</b>	CCDF of the capacity for a 4x8 system for a reuse factor of 7 (a) K=0 (b) K=10 . . . . .	52
<b>6.18</b>	CCDF of the capacity for a 4x8 system for a reuse factor of 7 and K=50 . . . . .	53

## ABSTRACT

The use of multiple antennas at both ends of a wireless link can provide substantial increases in capacity. In MIMO systems, the multiple antennas could be utilized in different ways to maximize the performance in a particular environment. Previously, a spatial multiplexing system was compared with a system that uses multiple antennas to perform adaptive beamforming. In this thesis, we evaluate the performance of a hybrid MIMO (H-MIMO) system where the antennas are used in a combination of these two modes. Through simulations, we show that, over a wide range of target outage probabilities and Ricean K factors, the hybrid systems can achieve higher efficiencies for users who are farther from the base station or, alternatively, can provide higher capacities to a larger percentage of users in a cell.

# Chapter 1

## INTRODUCTION

### 1.1 Motivation

Because of the ever-increasing demand for higher data rates, maximizing the spectral efficiency is of paramount importance in next-generation wireless systems. An effective step in this direction is the use of multiple antennas at the transmitter, at the receiver, or at both ends, that is, so-called multiple-input multiple-output (MIMO) systems (e.g., see [1]-[6]). In recent years, it has been shown that MIMO systems can be used for spatial multiplexing, providing the potential for a linear increase in capacity with the number of antennas (e.g., see [6]-[8]). Substantial gains have been verified through analysis and simulation in single-cell environments [9]-[10] as well as in multi-cell applications [11]-[14].

In MIMO systems, the multiple antennas could be utilized in different ways to maximize the performance in a particular environment. In [15], using a comprehensive simulation in a real-world cellular environment, a spatial multiplexing (SM) system was compared with a system that uses multiple antennas to perform adaptive beamforming (AB). Although SM is shown to be surprisingly robust, the results

in [15] also demonstrate different sensitivities to the degree of scattering in the environment and the target outage probabilities for the two schemes. In particular, as the environment becomes more specular in nature and as the outage requirement becomes more stringent, the spectral efficiency of the SM system decreases while the AB system improves due to the directive nature of beamforming.

## 1.2 Objective and Contributions

Because SM and AB systems exhibit different, essentially opposite, sensitivity to the scattering in the environment, an interesting possibility is to employ a hybrid MIMO (H-MIMO) system, where the antennas are used in a combination of the SM and AB modes. As we decrease the number of independent substreams so that more antennas are dedicated to AB, we obtain more power gain and cochannel interference suppression ability. This will stabilize the capacity variation in a cell, at the expense of maximum achievable capacity. Thus, in this hybrid system, there exists a trade-off between maximum achievable capacity and the stability of the capacity in a cell.

The objective of the research described here is to evaluate the performance of H-MIMO systems in different simulation environments and to compare these systems with more conventional SM and AB approaches.

Multiple antennas are a fundamental component of next generation wireless systems, especially cellular systems and wireless metropolitan and local area networks. In particular, both 4G cellular systems and next-generation wireless LANs, such as

the IEEE 802.11n standard, include MIMO techniques. In all of these systems, the primary driver is the higher data rates and spectral efficiencies necessary to provide seamless multimedia services to a large number of subscribers. Hybrid systems, as suggested here, offer the possibility to tailor the transmission arrangement to better meet the needs of a specific wireless link.

### **1.3 Outline of the Thesis**

In Chapter 2, we provide a brief overview of the radio environment, highlighting the important propagation phenomena encountered in wireless communications. In Chapter 3, we present a brief review of multiple antenna systems, describe algorithms for determining the optimal weights for combining the signals from different antennas, and summarize the information theoretic capacities for different antenna configurations. We describe the link and channel models in Chapter 4, and the interference model and receiver processing in Chapter 5. Simulation results are presented in Chapter 6, and conclusions and future work are discussed in Chapter 7.

### **1.4 List of Acronyms**

Several acronyms will be used throughout this thesis. The most important are summarized below. Each acronym will also be defined at least once in the text. In addition, throughout this thesis, we will use the following conventions:  $x$ ,  $\mathbf{x}$ , and  $\mathbf{X}$  denote a scalar, a vector, and a matrix, respectively.

**Table 1.1:** List of Acronyms

AB	Adaptive Beamforming
SM	Spatial Multiplexing
LOS	Line-of-Sight
NLOS	Non-Line-of-Sight
ISI	Intersymbol Interference
SVD	Singular Value Decomposition
SISO	Single-Input Single-Output
SIMO	Single-Input Multiple-Output
MISO	Multiple-Input Single-Output
MIMO	Multiple-Input Multiple-Output
SINR	Signal-to-Interference-plus-Noise-Ratio
H-MIMO	Hybrid MIMO
CCI	Cochannel Interference
MMSE	Minimum Mean Square Error
MSINR	Maximum Signal-to-Interference-plus-Noise Ratio
CCDF	Complementary Cumulative Distribution Function

## Chapter 2

# THE RADIO CHANNEL

In this chapter, we present a brief review of the radio environment to serve as a basis for the channel models discussed in Chapter 4. As the transmitted radio wave travels, it arrives at the destination through various physical mechanisms such as reflection, refraction, diffraction, and scattering. The most important phenomena, and those of most interest in this thesis, are path loss, shadow fading, and multipath fading. Each of these is briefly described next.

### 2.1 Path Loss

The path loss is defined as the ratio of the received power to the transmitted power and represents the mean attenuation experienced by the transmitted signal. Various models have been proposed to represent this loss (for example, see [16]-[18]). In free-space, the received signal power varies inversely with the square of the distance between the transmitter and receiver, that is, the path loss is

$$L = \frac{P_r}{P_t} = G_t G_r \left( \frac{\lambda}{4\pi d} \right)^2 \quad (2.1)$$

where  $P_r$  is the received power,  $P_t$  is the transmitted power,  $G_t$  is the gain of transmitting antenna,  $G_r$  is the gain of receiving antenna,  $\lambda$  is the wavelength of transmission, and  $d$  is the distance between the transmitter and receiver.

In a more realistic environment, due to factors such as reflection, refraction, and diffraction, the attenuation increases more rapidly with distance. Here, we take a simplified approach and model the path loss as [16]-[18]

$$L = \frac{P_r}{P_t} = \left(\frac{\lambda}{4\pi d_0}\right)^2 \left(\frac{d_0}{d}\right)^\gamma \quad (2.2)$$

where the first term represents the loss at a specified reference distance,  $d_0$ , and  $\gamma$  is the path-loss exponent, typically ranging from 2 to 4 in most cases of interest for cellular systems.

## 2.2 Shadow Fading

In addition, the transmitted signal is shadowed by obstructions such as hills and buildings. This gives rise to large-scale variations with respect to the local mean signal power. This shadowing is usually characterized with a lognormal distribution, that is, if the received signal power,  $s$ , is represented in decibels (dB) by  $S$ , then the probability density function of  $S$  is Gaussian [16]-[18],

$$p(S) = \frac{1}{\sqrt{2\pi\sigma_s^2}} \exp\left[-\frac{(S - \bar{S})^2}{2\sigma_s^2}\right] \quad (2.3)$$

where  $\bar{S}$  and  $\sigma_s^2$  are the mean and the variance of  $S$ , respectively.

## 2.3 Multipath Fading

In a typical wireless communication environment, rarely is there a direct line-of-sight path between the transmitter and receiver. Rather, propagation is mainly by way of scattering from the surfaces of buildings and objects. The transmitted signal arrives at the receiver via several paths simultaneously, with the various waves

arriving with different amplitudes and phases and different times of arrival. These signals combine vectorially at the receiving antenna to give a resultant signal, and they can reinforce (in-phase) or cancel each other (out-of-phase). The constructive and destructive interference results in a signal which varies with the distance between the transmitter and receiver. In particular, as a mobile moves, the received signal envelope fluctuates. These variations occur over short distances and the phenomenon is usually referred to as small-scale or fast fading (as opposed to the slow fading resulting from shadowing).

If there is no line-of-sight (LOS) component, the numerous rays add up to create a signal envelope,  $r$ , that follows a Rayleigh distribution [16]-[18] given by

$$p(r) = \frac{r}{\sigma^2} \exp\left[-\frac{r^2}{2\sigma^2}\right] \quad (2.4)$$

where  $2\sigma^2$  is the mean power of the multipath signal [16]. If there is a strong LOS component, the resultant signal envelope follows a Ricean distribution given by

$$p(r) = \frac{r}{\sigma^2} \exp\left[-\frac{r^2 + a^2}{2\sigma^2}\right] I_0\left(\frac{ar}{\sigma^2}\right) \quad (2.5)$$

$$I_0(x) = \frac{1}{2\pi} \int_0^{2\pi} \exp[x \cos\theta] d\theta \quad (2.6)$$

where  $I_0(x)$  is the modified Bessel function of the zeroth order and  $a$  is the signal amplitude from the deterministic LOS path.

In comparing the H-MIMO systems, an important parameter will be the ratio of the powers of the LOS component to the scattering or non-line-of-sight(NLOS) components, which we call the Ricean K factor,  $K = a^2/\sigma^2$  [19]. This is a measure



Figure 2.1: Radio environment

of the richness of the scattering environment. If the LOS component dominates, then the variations in the received signal envelope will be small. On the other hand, if  $a = 0$  (i.e., no LOS component), the channel reduces to a Rayleigh fading channel.

Now, the received signal power (in dB),  $S$ , which is spatially averaged over the multipath fading, can be represented by

$$S = \bar{S} + X \quad (2.7)$$

where  $\bar{S}$  is the median of the local average received signal power and  $X$  is the dB value of the lognormal shadow fading, which is Gaussian with zero mean and variance  $\sigma_s^2$ . Then, the *instantaneous* received signal power can be given as

$$s_{inst} = s(r^2/\bar{r}^2) \quad (2.8)$$

Note that the average of  $s_{inst}$  over multipath fading is precisely  $s$ . Now, in dB, we have

$$S_{inst} = \bar{S} + X + 10 \log (r^2/\bar{r}^2) \quad (2.9)$$

where  $r$  is Rayleigh or Ricean fading due to multipath. A simple illustration of the received signal power in a typical radio environment is shown in Figure 2.1. In presenting this brief overview, we have assumed that the transmitted signal does not undergo any spreading in time or frequency. Next, we describe the effects of delay spread (spreading in time) and Doppler (spreading in frequency).

## 2.4 Delay Spread

The received signal is composed of several discrete multipath components, each with different arrival times, magnitudes, and phases. The different times of arrival result in a received signal that is longer in time than the transmitted signal. This is called delay spread, which results in intersymbol interference (ISI). Depending on the transmission rate, this can result in a significant performance degradation [20].

A useful measure of the time spread of the channel is the root-mean-squared (rms) delay spread,  $\sigma_T$ , defined as

$$\sigma_T = \sqrt{\overline{T^2} - (\overline{T})^2} \quad (2.10)$$

where  $\overline{T}$  is the average delay and  $\overline{T^2}$  is the second moment of the delay.

The significance of the channel time dispersion, and the resulting ISI, depends on the relative values of the rms delay spread and the symbol period,  $T_s$ . If  $\sigma_T \ll T_s$ , then the ISI will be negligible and the variation in frequency over the bandwidth of the signal will be small (flat fading). Alternatively, if  $\sigma_T \gg T_s$ , then the ISI will be

significant and some compensation will be required. In the latter case, the channel will vary considerably over the signal bandwidth (frequency selective fading).

## 2.5 Doppler Spread

In mobile radio applications, the channel changes in time due to the motion of the transmitter and receiver, or even because of the movement of scatterers. The rate of change of the channel response can be well-approximated by the maximum Doppler frequency,  $f_m = \frac{v}{\lambda}$ , where  $v$  is the speed of the mobile [18]. As with the delay spread, the relative importance of the channel time variance is determined by the relationship of the Doppler frequency to the signal bandwidth. Equivalently, by defining a coherence time, a measure of the expected time duration over which the channel's response is essentially invariant, we can relate the channel time variation to the symbol period.

Using the coherence time,  $T_o$ , we can categorize fading as either fast or slow. If the channel coherence time is much shorter than the symbol time,  $T_s$ , then the channel changes several times during a symbol transmission period, which causes baseband signal distortion and makes channel estimation difficult. In this case, we say that the fading is fast ( $T_o \ll T_s$ ). On the other hand, a channel is said to be slowly fading if the channel changes slowly relative to the symbol period ( $T_o \gg T_s$ ). In this case, the channel response is constant over a symbol time.

## Chapter 3

# MULTIPLE ANTENNA SYSTEMS

### 3.1 Multiple Antenna Techniques

Multiple antennas at the transmitter, at the receiver, or at both ends of the communications link, can provide significant gains in performance. In this chapter, we describe the benefits of multiple antennas used in different arrangements: (1) at the receiver to provide diversity gain (Figure 3.1), (2) at both ends as an adaptive beamformer (Figure 3.2), and (3) to provide spatial multiplexing benefits (Figure 3.3). In addition, we provide the information-theoretic capacity for different antenna configurations.

#### 3.1.1 Spatial Diversity

As indicated in the previous chapter, in a wireless communication environment, a major limiting factor of performance is multipath fading in which the received signal experiences deep fades. The basic concept of diversity relies on the fact that a signal that is in a deep fade on one path is unlikely to experience a deep fade simultaneously on an independent radio path. There are several algorithms for combining the signals from the independent branches; selection combining, maximal ratio combining, and equal-gain combining are the most common [18].

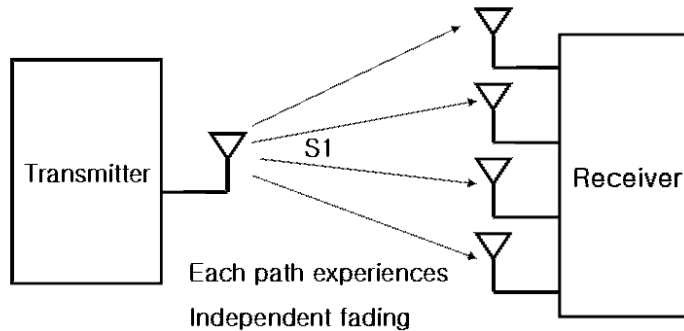


**Figure 3.1:** 1x4 diversity system

In selection diversity, the receiver selects the output of the antenna with the largest instantaneous SNR. In maximal ratio combining, the received signal on each antenna is amplitude- and phase-weighted and combined to maximize the output SNR of the composite signal. Using this approach, the output SNR is the sum of the SNRs on the individual branches. Equal-gain combining is slightly simpler; in this case, the received signals are only co-phased, not amplitude-weighted. For more details on diversity combining, see Chapter 5 in [18].

### 3.1.2 Adaptive Beamforming

Instead of diversity, the antennas can be configured to minimize the interference and noise level, or equivalently, to maximize the output signal-to-interference-plus-noise-ratio (SINR). In one realization of adaptive beamforming (AB), multiple antennas at both ends of the communications link create beam patterns in the direction of the desired users, thereby suppressing cochannel interference (CCI). This

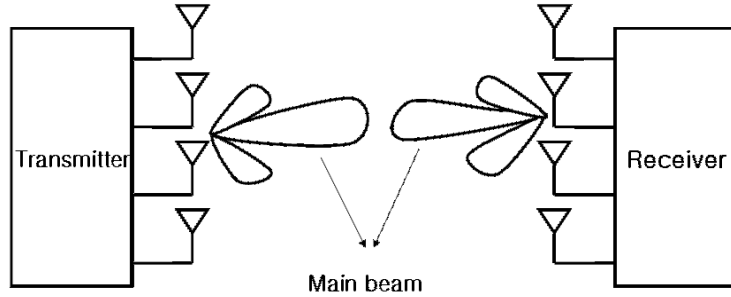


**Figure 3.2:** 4x4 beamforming system

reduction in CCI enables more aggressive frequency reuse which, in turn, enables an increase in the system capacity. In addition, AB can improve the noise performance by focusing the energy toward the intended users, instead of wasting it in other unnecessary directions, like an omni-directional antenna would [21]-[23]. The most commonly selected performance criteria for selecting the antenna weights are described in Section 3.3.

### 3.1.3 Spatial Multiplexing

In a spatial multiplexing scheme (SM), multiple antennas are employed at both ends of the communications link. At the transmit end, a high-rate bit stream is decomposed into a number of substreams with each substream transmitted over a different antenna. Each substream is encoded, modulated independently, and transmitted simultaneously over the same frequency band. At the receiver, the composite signals are detected and estimated while using the knowledge of the complex channel

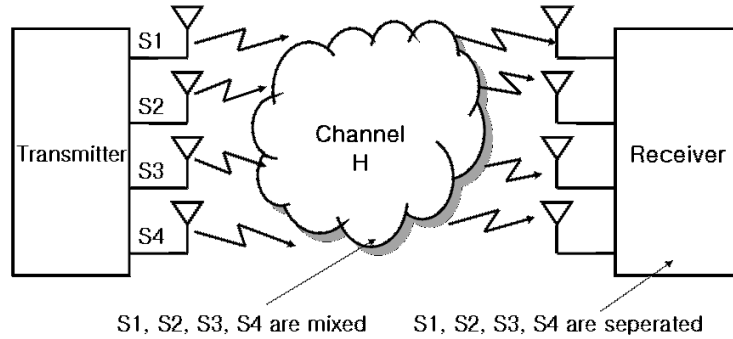


**Figure 3.3:** 4x4 spatial multiplexing system

gain matrix obtained through training. Finally, each separate substream is multiplexed at the receiver to yield the original high-rate bit stream [8].

A key concept in a SM system is the use of a parallel decomposition of the channel to obtain independent channels. By transmitting independent bit streams on non-interfering parallel channels, even on the same frequency band, we can separate each transmitted substream at the receiver. However, this parallel decomposition assumes that the channel has sufficient scattering to provide a matrix which is full rank. Under these conditions, the channel matrix can then be decomposed into the diagonal matrix of singular values over which independent streams are transmitted. As we show in the next section, SM can provide a substantial increase in capacity.

### 3.2 Multiple Antenna Information Theory

In this section, we present a summary of the information-theoretic capacity for multiple antenna systems. We start with a system with only a single antenna at

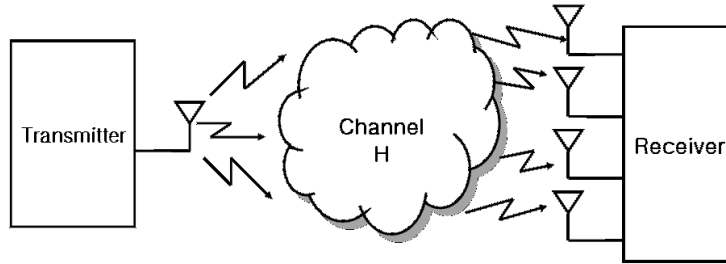


**Figure 3.4:** 1x4 SIMO system

the transmitter and receiver, a Single-Input Single-Output (SISO) system. Then, we describe systems with an array at only one side of the link, SIMO (Single-Input Multiple-Output) and MISO (Multiple-Input Single-Output) systems. Finally, we describe a MIMO (Multiple-Input Multiple-Output) system which employs antenna arrays at both the transmitter and receiver. Such a system can provide substantial gains in capacity. Figures 3.4, 3.5, and 3.6 show SIMO, MISO, and MIMO systems, respectively.

For a SISO system, the capacity is given by [24]

$$C = \log_2(1 + SNR|h|^2) \text{ bps/Hz}, \quad (3.1)$$

where  $h$  is the normalized complex channel gain, and  $SNR$  is the average signal-to-noise ratio. Since  $h$  is a random variable, the capacity is also a random variable. Note that  $SNR|h|^2$  represents the instantaneous SNR at the receiver. By introducing

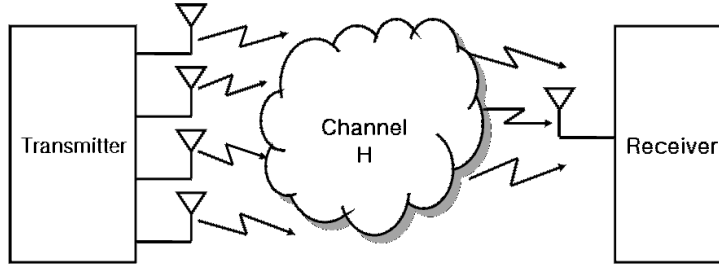


**Figure 3.5:** 4x1 MISO system

more antennas at the receiver, a SIMO configuration, we can obtain a capacity [6]

$$C_{SIMO} = \log_2(1 + SNR \sum_{i=1}^M |h_i|^2) \text{ bps/Hz} \quad (3.2)$$

where M is the number of receive antennas.

Comparing this configuration to SISO, we can see that a SIMO system provides an increase in capacity. The increase is logarithmic with the number of antennas and results because more receive antennas enable the collection of more energy (array gain) and the probability that the transmitted signal experiences a deep fade decreases (diversity gain).

Another possibility is to opt for transmit diversity, introducing N antennas at the transmitter with only one at the receiver (MISO). For this system, the capacity is given by [6]

$$C_{MISO} = \log_2(1 + \frac{SNR}{N} \sum_{i=1}^N |h_i|^2) \text{ bps/Hz} \quad (3.3)$$

where N is a normalization factor which ensures that the transmitted power is fixed so that a fair comparison is made. Using this approach, we have diversity gain but

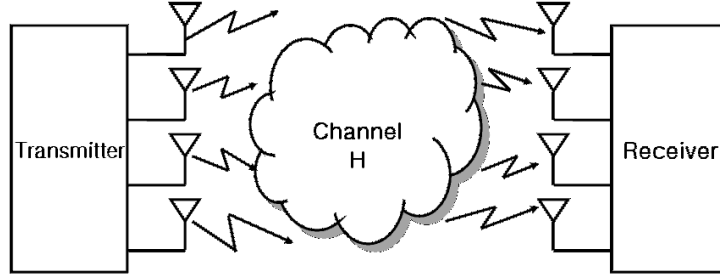


**Figure 3.6:** 4x4 MIMO system

no array gain.

Finally, we consider a MIMO system in which multiple antennas are used at both ends of the communications link. In this case, the capacity is given by [6]

$$C = \log_2 \left[ \det(\mathbf{I}_N + \frac{SNR}{M} \mathbf{H}\mathbf{H}^H) \right] \text{ bps/Hz} \quad (3.4)$$

where  $\mathbf{H}$  is the  $M \times N$  complex channel matrix with i.i.d channel gain elements, and  $\mathbf{I}_N$  represents an  $N \times N$  identity matrix. Performing a singular value decomposition (SVD) on the matrix  $\mathbf{H}$ , we get

$$\mathbf{H} = \mathbf{U}\mathbf{D}\mathbf{V}^H \quad (3.5)$$

where  $H$  denotes the conjugate transpose.  $\mathbf{D}$  is a diagonal matrix of real, nonnegative singular values (the square roots of the eigenvalues of  $\mathbf{H}\mathbf{H}^H$ ), and  $\mathbf{U}$  and  $\mathbf{V}$  are corresponding singular vectors. We perform precoding with the right singular vector, and postcoding with the left singular vector. Then, under the assumption

that the each eigenvalue is the same, the capacity equation is given by

$$C = \min(M, N) \log_2(1 + SNR) \text{ bps/Hz} \quad (3.6)$$

It is clear from (3.6) that without any power and bandwidth expansion, the capacity scales linearly with minimum of the number of transmit and receive antennas,  $\min(M, N)$ , providing a substantial increase in system capacity. This is referred to as spatial multiplexing gain.

### 3.3 Criteria for Optimal Weight Vectors

In this section, we review the common criteria for choosing the optimal receiver weights for both SM and AB. In general, the antenna array at the receiver tries to recover the original transmitted data stream in such a way in SM that it separates the substreams or, in AB, so that it optimally combines the received signals. Because of the time varying nature of the multipath channel, the receiver must also adapt by adjusting the weight vector. This is usually accomplished through training.

#### 3.3.1 Minimum Mean Square Error (MMSE) Criterion

The goal of this criterion is to minimize the mean-squared error (MSE) between the desired signal  $d$ , and the estimate of the desired signal  $\hat{d} = \mathbf{w}^H \mathbf{x}$ , where  $\mathbf{x}$  is the received signal vector across the receive antennas and  $\mathbf{w}$  represents the antenna weighting across the receive antennas. The error,  $e$ , in the detected signal is given by

$$e = d - \hat{d} = d - \mathbf{w}^H \mathbf{x} \quad (3.7)$$

The resulting MSE is then given by

$$J(\mathbf{w}) = E\{ee^*\} \quad (3.8)$$

where  $*$  denotes conjugation. The weight vector  $\mathbf{w}$  is chosen to minimize  $J(\mathbf{w})$ .

Expanding (3.8), we get

$$\begin{aligned} J(\mathbf{w}) &= E\{ee^*\} \\ &= E\{(d - \mathbf{w}^H \mathbf{x})(d^* - \mathbf{x}^H \mathbf{w})\} \\ &= E\{|d|^2 - d\mathbf{x}^H \mathbf{w} - \mathbf{w}^H \mathbf{x}d^* + \mathbf{w}^H \mathbf{x}\mathbf{x}^H \mathbf{w}\} \\ &= E\{|d|^2\} - E\{d\mathbf{x}^H\}\mathbf{w} - \mathbf{w}^H E\{\mathbf{x}d^*\} + \mathbf{w}^H E\{\mathbf{x}\mathbf{x}^H\}\mathbf{w} \end{aligned} \quad (3.9)$$

If we define the autocorrelation of  $\mathbf{x}$  as  $\mathbf{R}_x = E\{\mathbf{x}\mathbf{x}^H\}$  and the cross correlation between  $\mathbf{x}$  and  $d$  as  $\mathbf{p} = E\{\mathbf{x}d^*\}$ , (3.9) reduces to

$$J(\mathbf{w}) = E\{\sigma_d^2 - \mathbf{p}^H \mathbf{w} - \mathbf{w}^H \mathbf{p} + \mathbf{w}^H \mathbf{R}_x \mathbf{w}\} \quad (3.10)$$

where  $\sigma_d^2$  is a variance of the desired signal. The MSE in (3.10) is a quadratic function of  $\mathbf{w}$  and is convex; thus, it has unique minimum. In order to minimize the cost function, we take the derivative with respect to  $\mathbf{w}$  and set it to zero. After some manipulation, we obtain the optimum weight vector as

$$\mathbf{w}_{opt} = \mathbf{R}_x^{-1} \mathbf{p} \quad (3.11)$$

This is referred to as the Weiner solution [25].

### 3.3.2 Maximum Signal-to-Interference-plus-Noise-Ratio (MSINR) Criterion

In this performance criterion, the optimal receiver weights maximize the output SINR of the antenna array [26]. If we define  $\mathbf{x}$  as the received vector at the antenna array input, the received signal power after the beamforming process becomes

$$\begin{aligned}
\sigma_x^2 &= E\{|\mathbf{w}^H \mathbf{x}|^2\} \\
&= E\{(\mathbf{w}^H \mathbf{x})(\mathbf{w}^H \mathbf{x})^H\} \\
&= E\{\mathbf{w}^H \mathbf{x} \mathbf{x}^H \mathbf{w}\} \\
&= \mathbf{w}^H \mathbf{R}_x \mathbf{w}
\end{aligned} \tag{3.12}$$

where  $\mathbf{R}_x = E\{\mathbf{x} \mathbf{x}^H\}$  is the correlation matrix of the received vector. In the same fashion, let  $\mathbf{u}$  be the received interference-plus-noise vector at the array sensor input.

We define the interference-plus-noise power as

$$\begin{aligned}
\sigma_u^2 &= E\{|\mathbf{w}^H \mathbf{u}|^2\} \\
&= E\{(\mathbf{w}^H \mathbf{u})(\mathbf{w}^H \mathbf{u})^H\} \\
&= E\{\mathbf{w}^H \mathbf{u} \mathbf{u}^H \mathbf{w}\} \\
&= \mathbf{w}^H \mathbf{R}_{\text{int}} \mathbf{w}
\end{aligned} \tag{3.13}$$

where  $\mathbf{R}_{\text{int}} = E\{\mathbf{u}\mathbf{u}^H\}$  is the correlation matrix of the interference-plus-noise vector.

Using (3.12) and (3.13), the SINR becomes

$$SINR = \frac{\sigma_x^2}{\sigma_u^2} \quad (3.14)$$

$$= \frac{\mathbf{w}^H \mathbf{R}_x \mathbf{w}}{\mathbf{w}^H \mathbf{R}_{\text{int}} \mathbf{w}} \quad (3.15)$$

In order to maximize SINR, we differentiate (3.15) with respect to  $\mathbf{w}$ , and set it to zero. Then, we obtain

$$\begin{aligned} \mathbf{R}_x \mathbf{w} &= \frac{\mathbf{w}^H \mathbf{R}_x \mathbf{w}}{\mathbf{w}^H \mathbf{R}_{\text{int}} \mathbf{w}} \mathbf{R}_{\text{int}} \mathbf{w} \\ &= \lambda \mathbf{R}_{\text{int}} \mathbf{w} \end{aligned}$$

and

$$\mathbf{R}_{\text{int}}^{-1} \mathbf{R}_x \mathbf{w} = \lambda \mathbf{w} \quad (3.16)$$

Thus, we can find the optimum weight vector by solving the generalized eigenvalue problem in (3.16), where  $\lambda$  is the output SINR. Thus, maximization of SINR is equivalent to finding the largest eigenvalue of  $\mathbf{R}_{\text{int}}^{-1} \mathbf{R}_x$ , and the optimum weights are given as

$$\mathbf{w}_{opt} = P\{\mathbf{R}_{\text{int}}^{-1} \mathbf{R}_x\} \quad (3.17)$$

where  $P\{\}$  returns the largest eigenvector of the argument.

## Chapter 4

### LINK AND CHANNEL MODELS

In this chapter, the link and channel models used in the simulations are presented.

#### 4.1 Link Model for H-MIMO with Transmitter (Tx) Beamforming

In a SM system, the data stream is divided into  $N$  substreams, and each substream is transmitted over a different antenna using the same frequency band. At the receiver, the composite signal is received by  $M$  antennas, and the resulting  $M$ -dimensional signal vector is

$$\mathbf{r}_{\text{SM}} = \mathbf{H}\mathbf{x} + \mathbf{n} \quad (4.1)$$

Here,  $\mathbf{x}$  represents the  $N$ -dimensional transmitted signal vector,  $\mathbf{H}$  is the  $M \times N$  channel gain matrix, and  $\mathbf{n}$  is the  $M$ -dimensional noise vector with individual components modelled as zero-mean, unit-variance, complex Gaussian random variables.

In the AB system, a single data stream is transmitted over the  $N$  antennas, with a transmit beamforming weight vector  $\mathbf{w}$ . The  $M$ -dimensional signal vector at the receiver for this mode is given by

$$\mathbf{r}_{\text{AB}} = \mathbf{H}\mathbf{w}x + \mathbf{n} \quad (4.2)$$

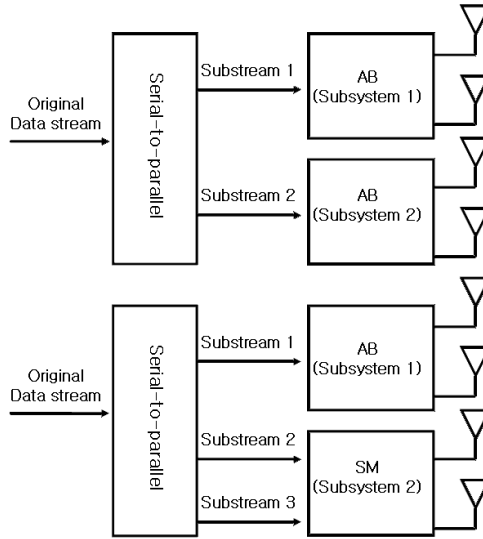


**Figure 4.1:** Hybrid system configurations for hybrid IS2 (upper) and hybrid IS3 (lower)

To guarantee a fair comparison, the total transmitted power is constrained to  $P$  in all cases. The transmit beamforming vector,  $\mathbf{w}$ , is determined using eigenbeamforming. In this method, the signal is transmitted through the channel with the largest path gain (largest eigenvalue). Thus,  $\mathbf{w}$  is simply the eigenvector corresponding to the largest eigenvalue of  $\mathbf{H}^H \mathbf{H}$ , with the norm set to unity [15].

We initially focus on a system with  $N=4$  transmit antennas and  $M=4$  receive antennas; the extension to more general system configurations is straightforward, and some examples will be given in Chapter 6. For  $N=M=4$ , there are four possibilities: Four transmitted substreams (pure SM); one transmitted substream on all four transmit antennas (pure AB); and two hybrid cases, namely, two and three

transmitted substreams. The two hybrid cases we analyze are shown in Figure 4.1. For the Hybrid IS2 (two independent substreams) system, the received signal vector is the combination of two AB signals and is given by

$$\mathbf{r}_1 = \mathbf{H}_1 \mathbf{w}_1 x_1 \quad (4.3)$$

$$\mathbf{r}_2 = \mathbf{H}_2 \mathbf{w}_2 x_2 \quad (4.4)$$

$$\mathbf{r}_{\text{IS2}} = \mathbf{r}_1 + \mathbf{r}_2 + \mathbf{n} \quad (4.5)$$

Here, the subscript  $\mathbf{i}$  is used for indexing the subsystems. For the Hybrid IS3 (three independent substreams) system, the received signal vector is a combination of SM and AB signals and is given by

$$\mathbf{r}_1 = \mathbf{H}_1 \mathbf{w}_1 x_1 \quad (4.6)$$

$$\mathbf{r}_2 = \mathbf{H}_2 \mathbf{x}_2 \quad (4.7)$$

$$\mathbf{r}_{\text{IS3}} = \mathbf{r}_1 + \mathbf{r}_2 + \mathbf{n} \quad (4.8)$$

## 4.2 Link Model for H-MIMO without Tx Beamforming

Here, we define an alternative link model where there is no transmit beamforming. In this case, the transmit beamforming weight  $\mathbf{w} = \mathbf{1}$ , and each antenna transmits exactly the same signal through the channel. This scheme is a simple transmit diversity system. Thus, in this case, we can define a hybrid of a SM system and a simple diversity system. We designate the simple diversity system as Div, and the hybrid of SM and Div as H-SMDiv.

For the SM system, the link model is the same as before. Thus, we only define link models for three cases: Div, wherein one stream is transmitted over the 4 antennas; H-SMDiv IS2, in which two substreams are transmitted with the corresponding Div subsystems; and H-SMDiv IS3, in which three substreams are transmitted, one for the Div subsystem and two for the SM subsystems.

For Div, the same data stream is transmitted on all of the transmit antennas. Then, the received signal vector at the mobile is given by

$$\begin{aligned}\mathbf{r}_{\text{Div}} &= \mathbf{h}_1x + \mathbf{h}_2x + \mathbf{h}_3x + \mathbf{h}_4x + \mathbf{n} \\ &= \sum_{k=1}^4 \mathbf{h}_kx + \mathbf{n}\end{aligned}\quad (4.9)$$

For H-SMDiv IS2, the received signal vector is defined as

$$\begin{aligned}\mathbf{r}_{\text{HSMDivIS2}} &= \mathbf{h}_1x_1 + \mathbf{h}_2x_1 + \mathbf{h}_3x_2 + \mathbf{h}_4x_2 + \mathbf{n} \\ &= \sum_{k=1}^2 \mathbf{h}_kx_1 + \sum_{k=3}^4 \mathbf{h}_kx_2 + \mathbf{n}\end{aligned}\quad (4.10)$$

Finally, we can represent the received signal vector for H-SMDiv IS3 as

$$\begin{aligned}\mathbf{r}_{\text{HSMDivIS3}} &= \mathbf{h}_1x_1 + \mathbf{h}_2x_1 + \mathbf{h}_3x_2 + \mathbf{h}_4x_3 + \mathbf{n} \\ &= \sum_{k=1}^2 \mathbf{h}_kx_1 + \mathbf{h}_3x_2 + \mathbf{h}_4x_3 + \mathbf{n}\end{aligned}\quad (4.11)$$

where  $\mathbf{h}_i$  represents channel gain vector from the  $i$ th transmit antenna to the receive antenna array and  $x_i$  is the transmitted signal (a scalar in this case).

### 4.3 Channel Model

In the simulations in this section, we use a Ricean fading channel model which takes into account both LOS and NLOS components. Using this model, we can control the richness of the scattering environment which strongly influences the performance of each system [15]. More specifically, the channel response is represented as [19]

$$\mathbf{H} = \sqrt{\frac{K}{K+1}} \mathbf{H}_{\text{LOS}} + \sqrt{\frac{1}{K+1}} \mathbf{H}_{\text{NLOS}} \quad (4.12)$$

where  $\mathbf{H}_{\text{LOS}}$  and  $\mathbf{H}_{\text{NLOS}}$  are  $M \times N$  channel matrices for the LOS (or specular) and scattering components, respectively, and where  $K$  is the ratio of the LOS and NLOS powers (called the Ricean  $K$  factor, as in Section 2.3). The respective channel matrices are given by

$$\begin{aligned} \mathbf{H}_{\text{NLOS}} &= \sqrt{G} \mathbf{Z} \\ \mathbf{H}_{\text{LOS}} &= \sqrt{G} \mathbf{a}(\theta_t) \mathbf{a}(\theta_r)^T \\ \sqrt{G} &= cd^{-\gamma} s \end{aligned} \quad (4.13)$$

where the elements of the  $M \times N$  matrix  $\mathbf{Z}$  are statistically independent, unit-variance, complex Gaussian random variables. The quantities  $\mathbf{a}(\theta_t)$  and  $\mathbf{a}(\theta_r)$  are the specular array response vectors at the transmitter and receiver, respectively. The gain  $G$  is determined by the distance between the base station and a mobile ( $d$ ), the path-loss exponent ( $\gamma$ ), and the lognormal shadow fading ( $s$ ). The constant  $c$  is a function of the carrier frequency and does not effect the comparison which follows.

Finally, we assume that the fading is flat over the bandwidth of interest, that is, there is no ISI. This corresponds to the condition  $\sigma_T \ll T_s$  in Section 2.4. For wider bandwidths, orthogonal frequency division multiplexing (OFDM) can be used

in conjunction with MIMO to counteract the frequency-selective fading. We also assume a quasi-static fading channel, so that there is time to adapt the antenna weights. This corresponds to the condition  $T_o \gg T_s$  in Section 2.5.

## Chapter 5

### SYSTEM MODEL AND RECEIVER PROCESSING

In this chapter, the interference model is described along with a discussion of the receiver processing. We consider downlink transmission in a multi-cell environment. We limit consideration to the nearest six cochannel cells, which usually dominate the system performance. We assume that sectorized antennas, with a half-power beamwidth of  $90^\circ$ , are used at the base stations, which are located at the centers of each cell.

#### 5.1 Cochannel Interference Condition

For the cochannel interference, we consider two different cases. In the first CCI scenario, referred to as CCI #1, the base stations in the cochannel cells are assumed to transmit the maximum number of independent substreams, that is, they operate in the SM mode. In the second CCI scenario, CCI #2, the base stations located in the desired cell and the cochannel cells operate in the same mode. For instance, if the desired base station adopts AB, then all cochannel base stations in the surrounding do the same.

For CCI #1, the received interference-plus-noise vector at the desired mobile unit is given by

$$\mathbf{r}_{\text{int}} = \sum_{k=1}^6 \mathbf{H}_k \mathbf{x}_k + \mathbf{n} \quad (5.1)$$

and, for CCI #2, it is

1. SM case:

$$\mathbf{r}_{\text{int}} = \sum_{k=1}^6 \mathbf{H}_k \mathbf{x}_k + \mathbf{n}$$

2. Hybrid IS3 case:

$$\mathbf{r}_{\text{int}} = \sum_{k=1}^6 \{ \mathbf{H}_{k1} \mathbf{w}_{k1} x_{k1} + \mathbf{H}_{k2} \mathbf{x}_{k2} + \mathbf{n} \}$$

3. Hybrid IS2 case:

$$\mathbf{r}_{\text{int}} = \sum_{k=1}^6 \{ \mathbf{H}_{k1} \mathbf{w}_{k1} x_{k1} + \mathbf{H}_{k2} \mathbf{w}_{k2} x_{k2} + \mathbf{n} \}$$

4. Adaptive beamforming case:

$$\mathbf{r}_{\text{int}} = \sum_{k=1}^6 \mathbf{H}_k \mathbf{w}_k x_k$$

Here,  $\mathbf{H}_{ki}$  is the channel gain matrix for the  $i$ th subsystem from the  $k$ th cochannel cell to the desired mobile, and  $\mathbf{w}_{ki}$  is the transmit weight beamforming vector for the  $i$ th AB subsystem at the  $k$ th cochannel base station. In both cases, the corresponding covariance matrix of the interference-plus-noise is

$$\mathbf{R}_{\text{int}} = E\{\mathbf{r}_{\text{int}} \mathbf{r}_{\text{int}}^H\} \quad (5.2)$$

## 5.2 Receiver Processing for Multiple Antenna Systems

In this section, we determine the optimal receiver weights for the receivers. For the purpose of recovering the transmitted signal, MMSE combining is assumed for all systems. In terms of performance, the MMSE combiner is superior to a zero-forcing receiver (ZF), but inferior to ordered successive interference cancellation (OSIC) -

MMSE [27]-[28]. However, in terms of system complexity, it lies between ZF and OSIC-MMSE. Thus, here, we choose MMSE; other criteria could be considered in future work.

### 5.2.1 Receiver Weighting for H-MIMO with Tx Beamforming

The MMSE receiver weighting in the SM mode is

$$\mathbf{W}_r = (\mathbf{H}\mathbf{H}^H + \mathbf{R}_{\text{int}})^{-1}\mathbf{H}^H \quad (5.3)$$

where  $\mathbf{W}_r$  is the matrix, in which each column consists of the receiver weight vector to separate each transmitted substream.

The corresponding receiver weighting in the AB mode is

$$\mathbf{w}_r = (\mathbf{R}_d + \mathbf{R}_{\text{int}})^{-1}\mathbf{H}\mathbf{w} \quad (5.4)$$

where

$$\mathbf{R}_d = \mathbf{H}\mathbf{w}\mathbf{w}^H\mathbf{H}^H \quad (5.5)$$

Similarly, for Hybrid IS2 and IS3 systems, the MMSE receiver weights are as follows:

Hybrid IS2:

$$\begin{aligned} \mathbf{w}_{ri} &= (\mathbf{R}_{d1} + \mathbf{R}_{d2} + \mathbf{R}_{\text{int}})^{-1}\mathbf{H}_i\mathbf{w}_i \\ \mathbf{R}_{di} &= \mathbf{H}_i\mathbf{w}_i\mathbf{w}_i^H\mathbf{H}_i^H, \quad i = 1, 2 \end{aligned} \quad (5.6)$$

Hybrid IS3:

$$\begin{aligned} \mathbf{w}_{r1} &= (\mathbf{R}_{d1} + \mathbf{R}_{d2} + \mathbf{R}_{\text{int}})^{-1}\mathbf{H}_1\mathbf{w}_1 \\ \mathbf{w}_{r2,3} &= (\mathbf{R}_{d1} + \mathbf{R}_{d2} + \mathbf{R}_{\text{int}})^{-1}\mathbf{H}_2 \end{aligned} \quad (5.7)$$

where

$$\mathbf{R}_{d1} = \mathbf{H}_1\mathbf{w}_1\mathbf{w}_1^H\mathbf{H}_1^H \quad (5.8)$$

and

$$\mathbf{R}_{d2} = \mathbf{H}_2 \mathbf{H}_2^H \quad (5.9)$$

### 5.2.2 Receiver Weighting for H-MIMO without Tx Beamforming

In this section, we determine the receiver weight vector for SM, Div, and two hybrids of SM and Div (when there is no transmitter beamforming). For the SM system, the receiver weight vector is the same as in the previous case. The receiver weights for Div, H-SMDiv IS2, and H-SMDiv IS3 are as follows:

Div:

$$\mathbf{w}_r = (\mathbf{R}_d + \mathbf{R}_{\text{int}})^{-1} \mathbf{h}_{\text{sum}} \quad (5.10)$$

where

$$\mathbf{h}_{\text{sum}} = \mathbf{h}_1 + \mathbf{h}_2 + \mathbf{h}_3 + \mathbf{h}_4 \quad (5.11)$$

and

$$\mathbf{R}_d = \mathbf{h}_{\text{sum}} \mathbf{h}_{\text{sum}}^H \quad (5.12)$$

H-SMDiv IS2:

$$\mathbf{w}_{r1} = (\mathbf{R}_{d1} + \mathbf{R}_{d2} + \mathbf{R}_{\text{int}})^{-1} \mathbf{h}_{\text{sum1}} \quad (5.13)$$

$$\mathbf{w}_{r2} = (\mathbf{R}_{d1} + \mathbf{R}_{d2} + \mathbf{R}_{\text{int}})^{-1} \mathbf{h}_{\text{sum2}} \quad (5.14)$$

where

$$\mathbf{h}_{\text{sum1}} = \mathbf{h}_1 + \mathbf{h}_2 \quad (5.15)$$

$$\mathbf{h}_{\text{sum2}} = \mathbf{h}_3 + \mathbf{h}_4 \quad (5.16)$$

and

$$\mathbf{R}_{d1} = \mathbf{h}_{\text{sum1}} \mathbf{h}_{\text{sum1}}^H \quad (5.17)$$

$$\mathbf{R}_{d2} = \mathbf{h}_{\text{sum2}} \mathbf{h}_{\text{sum2}}^H \quad (5.18)$$

H-SMDiv IS3:

$$\mathbf{w}_{r1} = (\mathbf{R}_{d1} + \mathbf{R}_{d2} + \mathbf{R}_{\text{int}})^{-1} \mathbf{h}_{\text{sum1}} \quad (5.19)$$

$$\mathbf{w}_{r2,3} = (\mathbf{R}_{d1} + \mathbf{R}_{d2} + \mathbf{R}_{\text{int}})^{-1} \mathbf{H}_2 \quad (5.20)$$

where

$$\mathbf{h}_{\text{sum1}} = \mathbf{h}_1 + \mathbf{h}_2 \quad (5.21)$$

$$\mathbf{H}_2 = [\mathbf{h}_3, \mathbf{h}_4] \quad (5.22)$$

and

$$\mathbf{R}_{d1} = \mathbf{h}_{\text{sum1}} \mathbf{h}_{\text{sum1}}^H \quad (5.23)$$

$$\mathbf{R}_{d2} = \mathbf{H}_2 \mathbf{H}_2^H \quad (5.24)$$

In all cases, we will assume that the channel matrix or vector is perfectly estimated at the receiver.

## Chapter 6

### SIMULATION RESULTS AND DISCUSSION

In this chapter, we present results that show the performance of each of the systems described in Chapters 4 and 5. We initially focus on a 4x4 system and use the following parameters: path-loss exponent = 3.5, lognormal shadowing with standard deviation = 8 dB, and a median received SNR = 25 dB at the cell boundary. First, we present the spectral efficiency (in bps/Hz) that a given percentage of users can achieve or exceed as a function of the distance from the base station. We then provide the complementary cumulative distribution function (CCDF) of the spectral efficiency, which is a good measure of the system-level performance of each approach.

#### 6.1 Capacity Evaluation

The spectral efficiency is computed for the four systems using the Shannon capacity. First, a channel matrix is generated and then the SINR is determined from

$$SINR_i = \mathbf{w}_{ri}^H \mathbf{R}_{\mathbf{x}_i} \mathbf{w}_{ri} / \mathbf{w}_{ri}^H \mathbf{R}_{\mathbf{int}} \mathbf{w}_{ri} \quad (6.1)$$

where  $\mathbf{i}$  indicates the independent substream,  $\mathbf{R}_{\mathbf{x}_i}$  is the covariance matrix of the  $i$ th received substream, and  $\mathbf{R}_{\mathbf{int}}$  is the received interference-plus-noise covariance

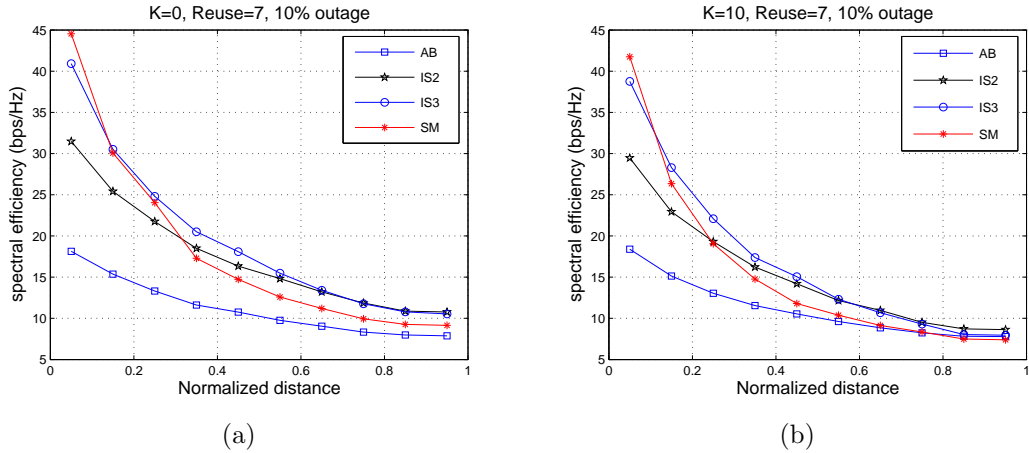


**Figure 6.1:** Outage capacity versus distance for CCI #1 for a reuse factor of 7 and outage=10% (a) K=0 (b) K=10

matrix. The capacity for each substream is calculated using the well-known formula,

$$C_i = \log_2(1 + SINR_i) \quad (6.2)$$

and the net capacity is derived as the sum of the capacities of the individual substreams, that is,

$$C_{sum} = \sum_{i=1}^k C_i \quad (6.3)$$

where  $k$  is the number of independent substreams in the system.

## 6.2 Capacity Versus Distance for CCI #1

In this simulation, mobiles are uniformly distributed in a hexagonal cell. We consider ten base-to-user distance regions for the cell, namely,  $[-0.1 + 0.1k]d_{max} < [0.1k]d_{max}$  with  $k=1$  to 10 and where  $d_{max}$  is the maximum distance in each cell. In each of these regions, we find the capacity that is achieved or exceeded for a fraction  $(1 - p_o)$  of all users, where  $p_o$  is the target outage probability. We use  $p_o = 0.1$  in

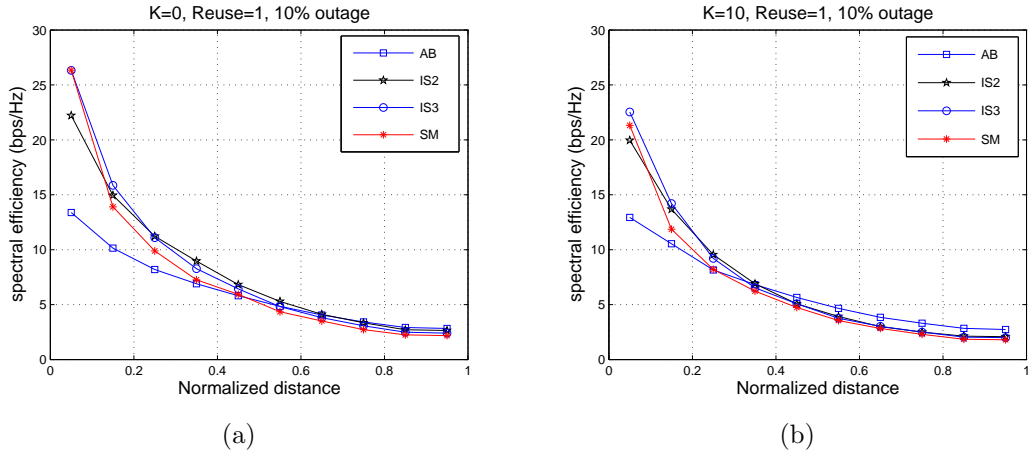


**Figure 6.2:** Outage capacity versus distance for CCI #1 for a reuse factor of 1 and outage=10% (a)  $K=0$  (b)  $K=10$

our calculations (10% outage), and we call the capacity for this outage the *outage capacity*. Results are shown in Figures 6.1 for two values of the Ricean  $K$  factor (0, Rayleigh fading, and 10) and a reuse factor of 7.

When the mobile unit is close to the base station, the SINR is usually quite high, and the SM mode (transmitting the maximum number of independent substreams) will be the most efficient. However, the capacity using SM degrades rapidly as the mobiles move away from the base station. Thus, if we introduce some power gain at the expense of maximum capacity, such as in the Hybrid IS2 and IS3 systems, then this variation over the cell can be reduced and, in turn, the outage performance improved. This is illustrated in Figure 6.1a where the hybrid systems provide a higher capacity than SM over a large part of the cell. The  $K$  factor in this figure is 0, giving the maximum scattering and the most advantageous conditions for SM. In the extreme case where only one substream is transmitted (the AB mode), the

variation over the cell is small but the capacity is also much lower than for the other approaches.

### **6.2.1 The impact of Ricean K factor**

As the Ricean K factor increases from 0 to 10 in Figure 6.1 for a reuse factor of 7, the degree of the scattering richness decreases. This decrease in scattering richness results in a performance degradation for SM. However, we observe that the performance of the AB system is pretty much the same as before. Actually, it improves a little at high K since we have more directivity resulting from a decrease in the scattering richness. Thus, the capacity curves for AB and SM cross each other between 0.2 and 0.3 in normalized distance, and AB shows slightly better performance than SM.

Moreover, we notice that the capacity for the hybrid systems is worse than before. The reason is as follows: In the case of Hybrid IS2, as the scattering richness decreases, each AB subsystem has more power gain, but this also means that self-interference, which is the interference among substreams in a system, is also increased. Thus, the increases in both the power gain and the self-interference effectively offset each other, resulting in a net performance degradation. Similar arguments apply to the Hybrid IS3 system.

### **6.2.2 The impact of reuse factor**

We have also performed the simulations with different reuse factors. The results are shown in Figure 6.2 for a reuse factor of 1. As the reuse factor is decreased,

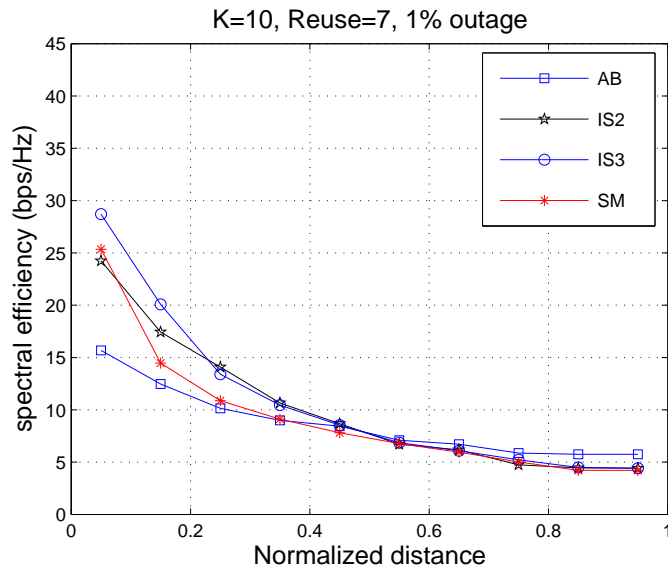


**Figure 6.3:** Outage capacity versus distance for CCI #1 for a reuse factor of 7, outage=1%, and K=10

and equivalently the distance between the cochannel cells is decreased, the per-cell performance of all the systems, as expected, degrades. In this case, the AB system has slightly better performance as the mobile moves farther from the base station due to the larger power gain. In reading these and subsequent results, some important factors to keep in mind are the following: (1) Whereas per-user capacity increases with reuse factor, the overall *system* capacity will be highest for reuse =1 (see [15]). (2) The capacity results shown in the figures will be lower for smaller values of median SNR at the cell boundary. (3) In reduction to practice the signal constellation size required for a given capacity will relate inversely to the number of independent signal streams, which militates in favor of using SM.

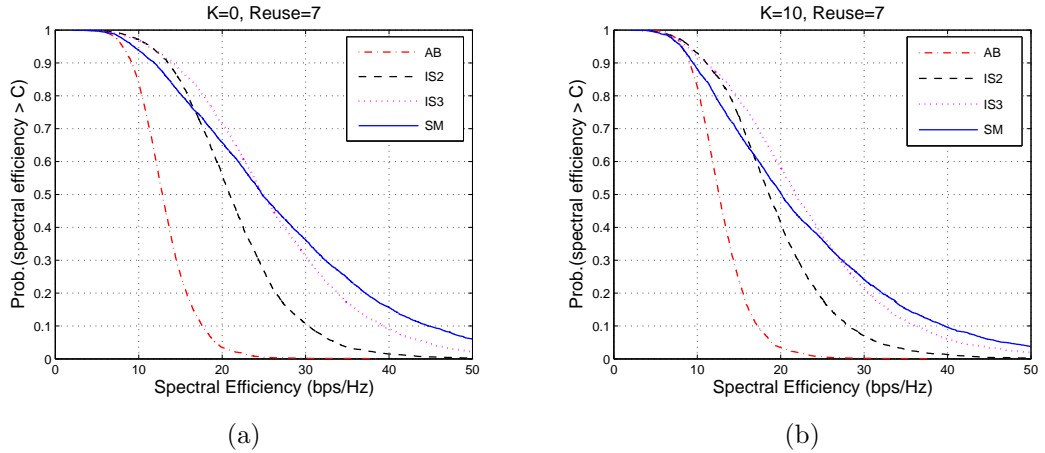


**Figure 6.4:** CCDF of the capacity for CCI #1 for a reuse factor of 7 (a)  $K=0$  (b)  $K=10$

### 6.2.3 The impact of target outage probability

As discussed previously, the target outage performance of the hybrid systems is improved over an SM system. We can clearly see this behavior by comparing Figures 6.1 (10% outage) and 6.3 (1% outage). As the target outage is reduced from 10% to 1%, the capacity offered by the SM mode around the base station is significantly reduced (17 bps/Hz). However, for the Hybrid IS3 and IS2 systems, the capacities are only decreased by 10 bps/Hz and 6 bps/Hz, respectively.

### 6.3 Capacity Distribution for CCI #1

Here, the goal is to determine what fraction of users in a cell achieve or exceed a given capacity. In this simulation, the mobiles are uniformly distributed in a cell, the capacity of each user is evaluated, and the CCDF is computed. Results are shown in Figure 6.4 for a reuse factor of 7, and two values of the Ricean  $K$  factor: 0 and 10. The results illustrate that hybrid systems can provide higher spectral

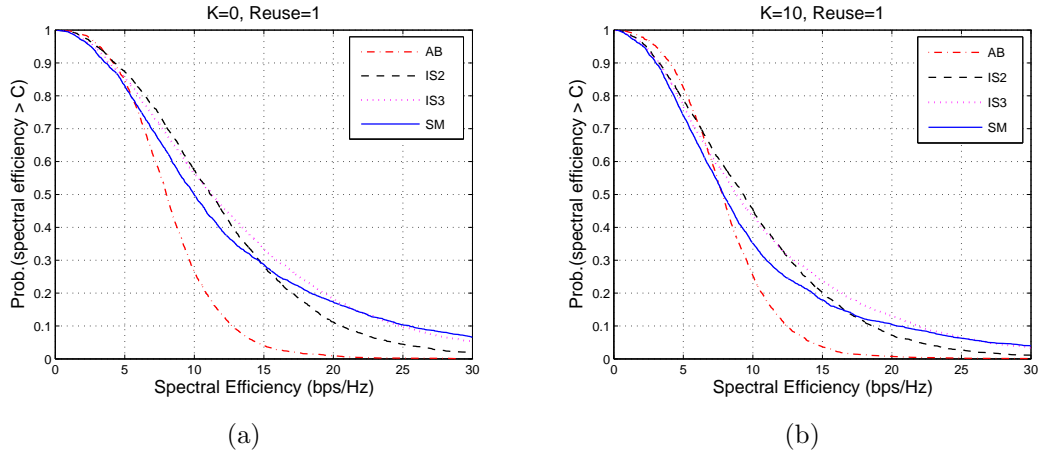


**Figure 6.5:** CCDF of the capacity for CCI #1 for a reuse factor of 1 (a)  $K=0$  (b)  $K=10$

efficiencies to more users in a cell. However, the highest capacities are still achieved using the SM mode. For example, from Figure 6.4a, with a  $K$  factor of 0, a capacity of 20 bps/Hz can be achieved by 70% of the users in a cell if the Hybrid IS3 system is used, but only 65% using the SM mode and 60% using the Hybrid IS2 system. To attain a higher capacity, say 30 bps/Hz, more independent substreams (SM or Hybrid IS3) are required. For very low outages, say 10% or less (90% CCDF), both hybrid systems slightly outperform the SM system.

### 6.3.1 The impact of Ricean $K$ factor

As the  $K$  factor increases from 0 to 10 (Figure 6.4b), the degree of scattering richness decreases, and, as discussed previously, the performance of all of the systems which use more than one independent substream degrades. The hybrid systems are now better than the SM system over a larger percentage of the cell. If we increase the Ricean  $K$  to 50 (Figure 6.6), we see that the performance of SM degrades the

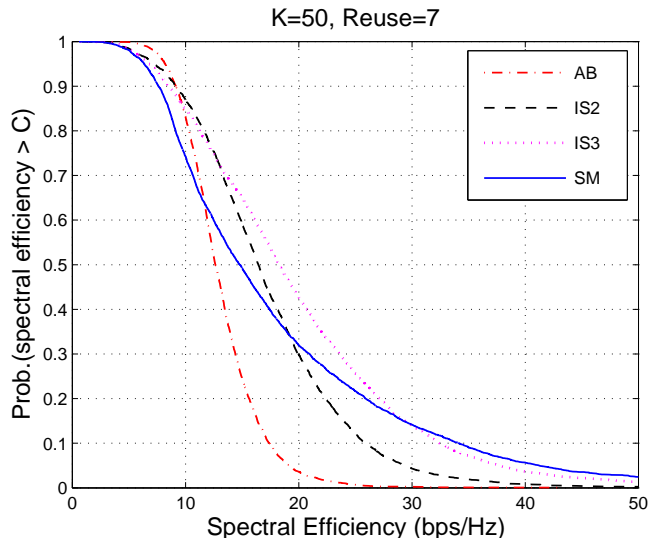


**Figure 6.6:** CCDF of the capacity for CCI #1 for a reuse factor of 7 and  $K=50$  most, and the hybrid systems are much better. In particular, the Hybrid IS3 system is better than the SM mode over 85% of the cell and the Hybrid IS2 is better than SM over almost 70% of the cell.

In order to observe the more general behavior of the systems as a function of Ricean  $K$  factor, we performed simulations for reuse factor=7, median SNR=25 dB, outage=10% and 50%, and varied  $K$  from 0 to 500. Here, results are presented in Figure 6.7. The performance of the SM and hybrid systems, as expected, degrades with Ricean  $K$ . On the other hand, the AB system improves slightly with  $K$  for both outage cases. We can clearly see that the hybrid systems are almost always better for large values of  $K$ .

### 6.3.2 The impact of reuse factor

We also performed the simulation with a reuse factor of 1 (Figure 6.5). As we

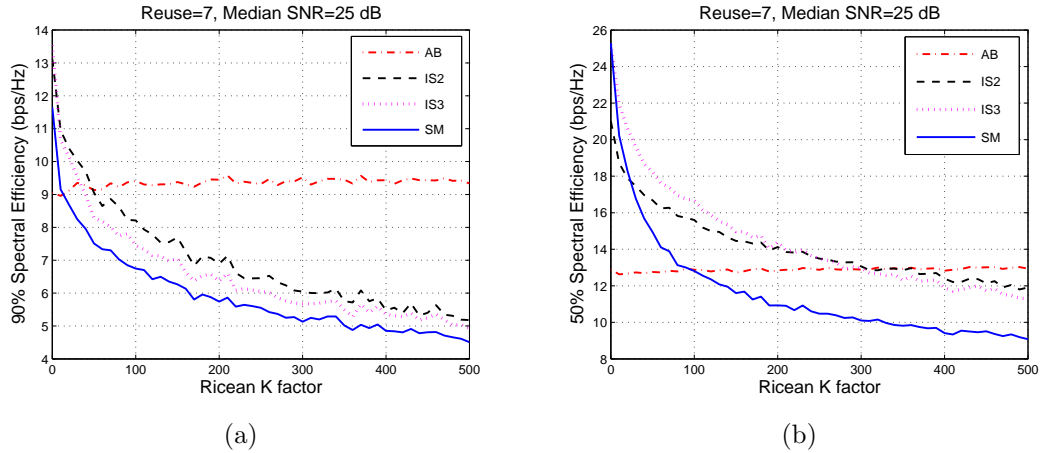


**Figure 6.7:** 90% and 50% (median) capacity as a function of Ricean K factor explained previously, the per-cell performance of all systems is degraded as the reuse factor decreases; however, the performance gap between the hybrid and SM systems also decreases. Nevertheless, the hybrid systems are better than the SM mode over a larger percentage of the cell. We also see that the AB system is now slightly better than the others for a K factor of 10 in low target outage regions.

### 6.3.3 The impact of median SNR

Here, we present the simulation results as a function of median SNR for a reuse factor of 7, the 90% capacity value, and Ricean K factors of 0 and 10. Results are shown in Figure 6.8. As expected, all of the systems tend to improve as the median SNR increases. In particular, the 90% capacity offered by all of the systems increases roughly linearly with median SNR between 0 to 20 dB. However, as the median SNR approaches 20-30 dB, the 90% capacity stops increasing with median SNR and becomes essentially flat. This is due to the fact that as the median SNR

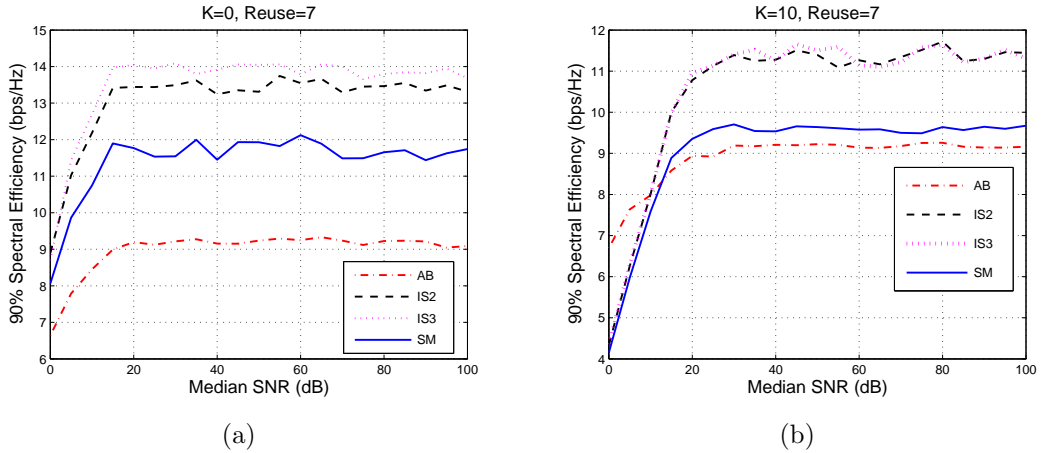


**Figure 6.8:** 90% capacity as a function of median SNR at the cell boundary for a reuse factor of 7 (a)  $K=0$  (b)  $K=10$

increases, additive thermal noise becomes unimportant compared to interference.

### 6.3.4 The impact of the number of cochannel interferers

For all of the results presented so far, we have assumed that all of the cochannel base stations operate in the SM mode and transmit the maximum number of independent substreams ( $k = 4$ ). We can also reduce the number of independent substreams that the interfering base stations use and observe the effect on performance. Results are shown in Figure 6.9 for the case where the cochannel base stations transmit only one independent substream with a reuse factor of 7 and  $K = 10$ . It is clear from the figure that, as the number of interfering streams decreases, the performance of the AB, Hybrid IS2, and Hybrid IS3 systems tend to improve. On the other hand, as expected, the performance in the SM mode does not change. In particular, the Hybrid IS3 system is better than the SM mode over 75% of the

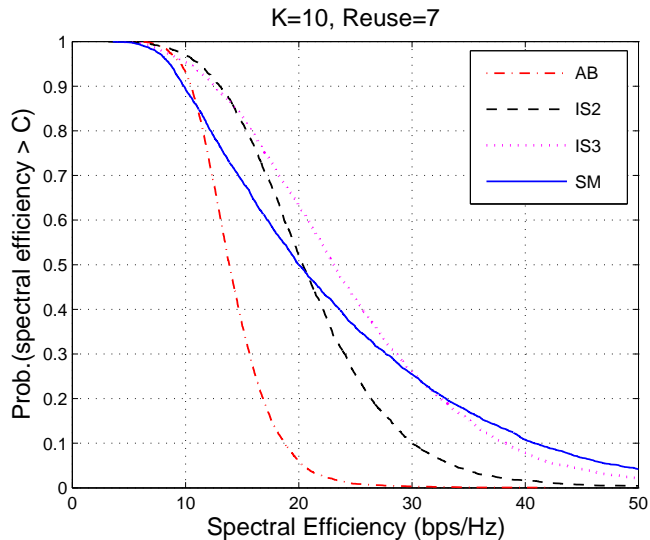


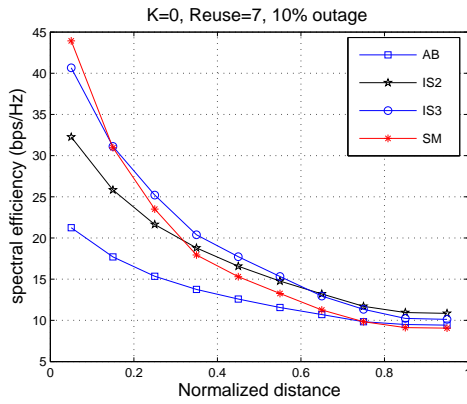
**Figure 6.9:** CCDF of the capacity for CCI #1 when cochannel base stations transmit only one substream for a reuse factor of 7 and  $K=10$

cell and the Hybrid IS2 is better over 50% of the cell.

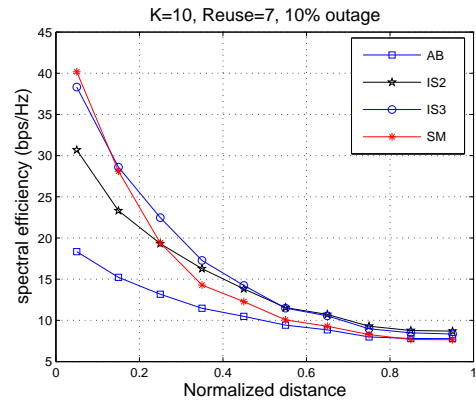
#### 6.4 Capacity Versus Distance for CCI #2

In this case, called CCI #2, the base stations located in the desired and cochannel cells all operate in the same mode. Figure 6.10 shows capacity versus distance plots. We notice that the Hybrid IS2, IS3, and SM systems show the same tendencies as in CCI #1, but the AB system shows an increase in capacity, especially for  $K=0$ .

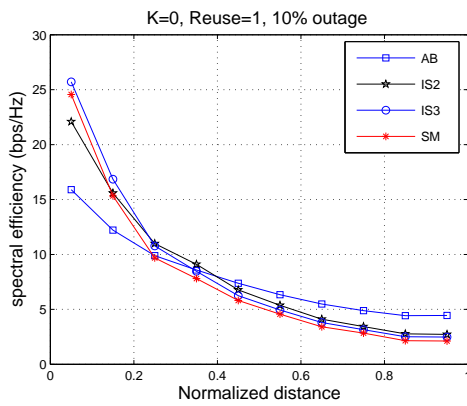
For CCI #1, as  $K$  increases, the performance of the AB system increases. However, for CCI #2, the opposite occurs. This is due to the fact that as the scattering richness decreases, the interference power coming from other base stations increases, because those base stations are also in the AB mode.



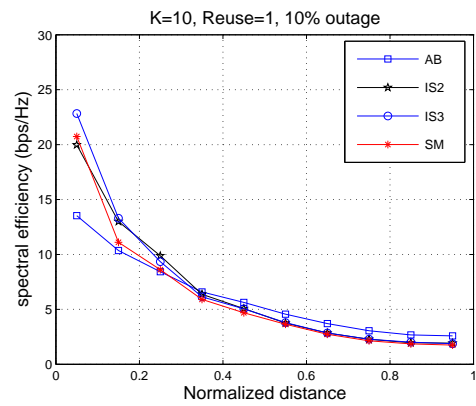
(a)



(b)



(c)



(d)

**Figure 6.10:** Outage capacity versus distance for CCI #2 (a)  $K=0$ , Reuse=7, (b)  $K=10$ , Reuse=7, (c)  $K=0$ , Reuse=1, (d)  $K=10$ , Reuse=1

**Table 6.1:** Mean achievable spectral efficiency for CCI #1

	Reuse = 1		Reuse =7	
	<b>K=0</b>	<b>K=10</b>	<b>K=0</b>	<b>K=10</b>
SM	12.84	10.13	27.10	22.75
Hybrid IS3	13.33	11.00	26.16	22.98
Hybrid IS2	13.14	10.27	21.56	19.22
AA	8.38	8.11	13.25	12.93

**Table 6.2:** Mean achievable spectral efficiency for CCI #2

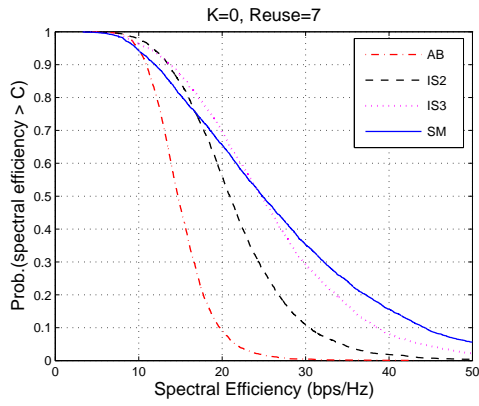
	Reuse = 1		Reuse =7	
	<b>K=0</b>	<b>K=10</b>	<b>K=0</b>	<b>K=10</b>
SM	12.84	10.12	27.09	22.92
Hybrid IS3	12.93	10.64	25.76	22.58
Hybrid IS2	11.98	10.03	21.72	19.04
AA	10.08	8.23	15.13	12.94

## 6.5 Capacity Distribution for CCI #2

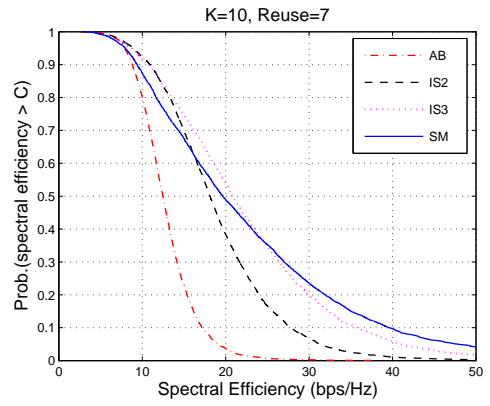
Here, we performed simulations on the capacity distribution for CCI #2. Corresponding results are shown in Figure 6.11. As in the previous section, for  $K=0$ , the spectral efficiency of the AB system is improved. On the other hand, the performance of the hybrid systems remains almost the same. Obviously, because the CCI scenario has not changed, the performance of the SM system does not change. Thus, up to 75%, the AB system provides better performance in terms of spectral efficiency which was not the case for CCI #1. As the Ricean  $K$  factor increases, the performance of all the systems degrades, for the same reasons as discussed above.

## 6.6 Mean Spectral Efficiency

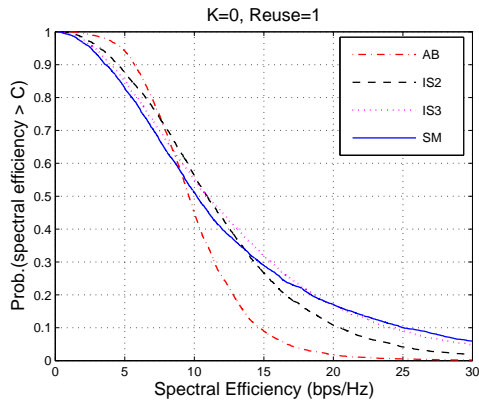
In Tables 6.1 and 6.2, we show the mean spectral efficiency for CCI #1 and CCI #2, respectively. For CCI #1, the Hybrid IS3 scheme offers more mean spectral



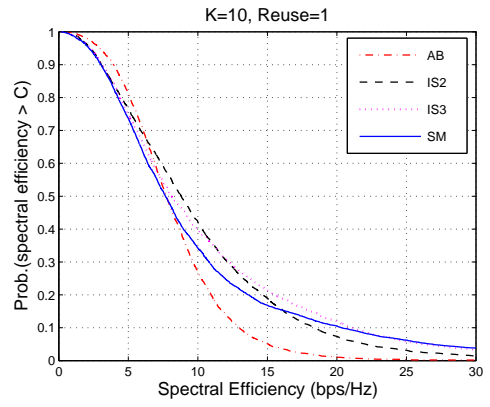
(a)



(b)



(c)



(d)

**Figure 6.11:** CCDF of the capacity for CCI #2 (a)  $K=0$ , Reuse=7, (b)  $K=10$ , Reuse=7, (c)  $K=0$ , Reuse=1, (d)  $K=10$ , Reuse=1

efficiency than the others since, as we can see in the corresponding CCDF plots (Figures 6.4 and 6.5), this scheme provides more spectral efficiency over a larger percentage of the cell than the SM mode. For CCI #2, the spectral efficiency provided by the SM and Hybrid IS3 schemes are almost the same. However, as we can see in the corresponding CCDF plots (Figures 6.11), the Hybrid IS3 scheme shows better performance in the low outage region. Thus, if the target outage is low, the Hybrid IS3 scheme might be favored.

### 6.7 No Transmitter Beamforming

In the previous results, it was assumed that eigenbeamforming was used at the transmitter. This requires that accurate channel state information be available (based on feedback from the mobile). Here, we consider the case when there is no transmitter beamforming (i.e.,  $\mathbf{w} = \mathbf{1}$ ). Results are shown in Figure 6.12. In comparing these results with those in Figure 6.8, we see that, as expected, the capacity of the AB and hybrid systems degrades. Nevertheless, the degradation is minimal and the benefit of not requiring feedback from the mobiles is significant.

### 6.8 Capacity Distribution for an 8x8 System

All of the previous results were for a system with 4 transmit and 4 receive antennas. In this section, we present simulation results for an 8x8 system, that is, 8 transmit and 8 receive antennas. Accordingly, there can be up to 8 independent substreams. Here, we consider 1, 2, 4, 6, and 8 substreams. Figure 6.13 shows the results for a

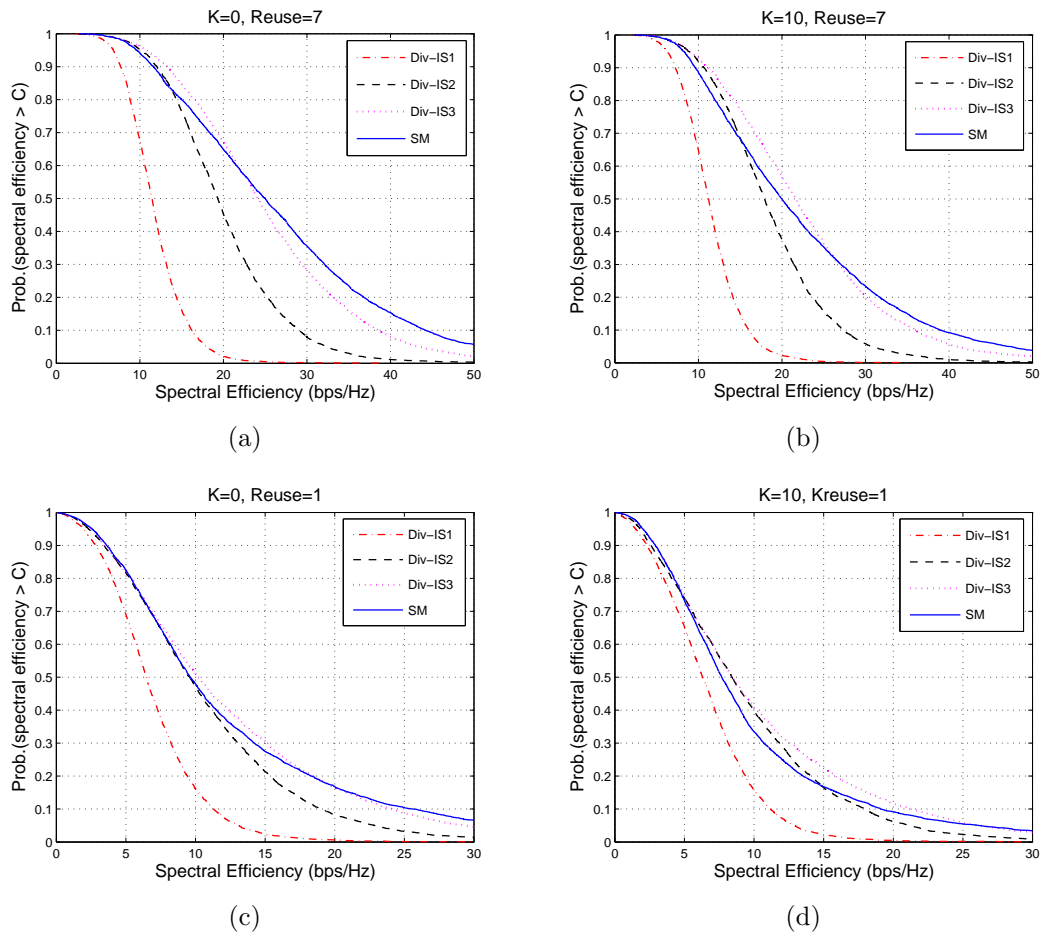


**Figure 6.12:** CCDF of the capacity with no transmitter beamforming (a)  $K=0$ , Reuse=7, (b)  $K=10$ , Reuse=7, (c)  $K=0$ , Reuse=1, (d)  $K=10$ , Reuse=1

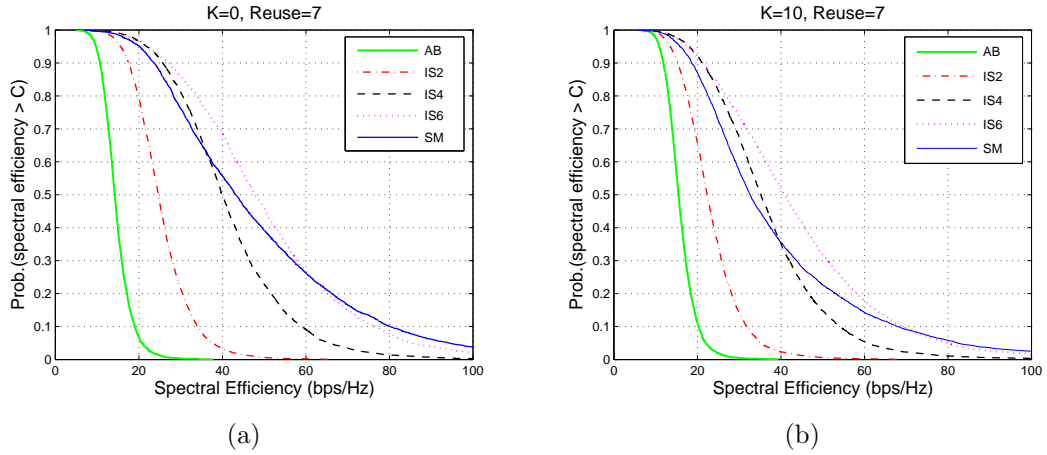


**Figure 6.13:** CCDF of the capacity for an 8x8 system for a reuse factor of 7 (a) K=0 (b) K=10

reuse factor of 7 and Ricean K factors of 0 and 10. We assume that each cochannel base station transmits 8 independent substreams (CCI #1).

As expected, as we increase the number of antennas, the performance of all of the systems is improved. However, we also notice that the performance gap between the hybrid systems and the SM system has increased compared with the 4x4 case. In the pure Rayleigh fading case (K=0), the Hybrid IS6 system provides higher efficiencies than the SM mode over 75% of the cell, and for a K factor=10, the Hybrid IS6 system is better over 90% of the cell. From Figure 6.13, 40 bps/Hz spectral efficiency can be achieved by 50% of the users if we use Hybrid IS6, but only 33 bps/Hz using the SM mode. If we increase K to 50 (Figure 6.14) then we see that the hybrid systems, especially Hybrid IS4 and Hybrid IS6, provide high spectral efficiency over a larger percentage of a cell than SM.

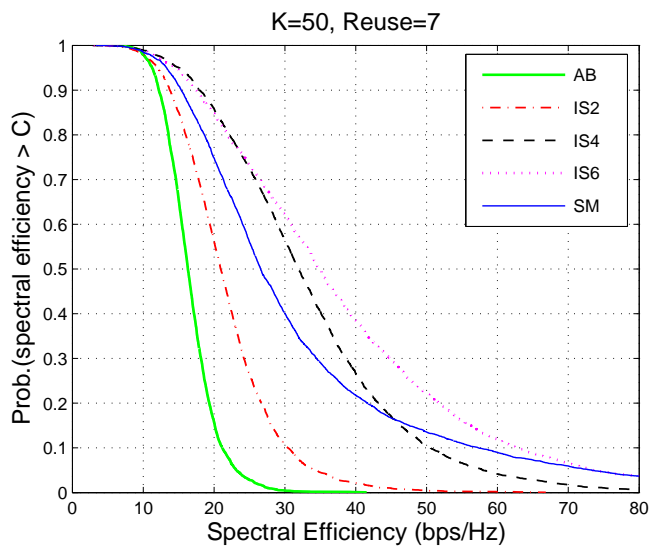


**Figure 6.14:** CCDF of the capacity for an 8x8 system for a reuse factor of 7 and  $K=50$

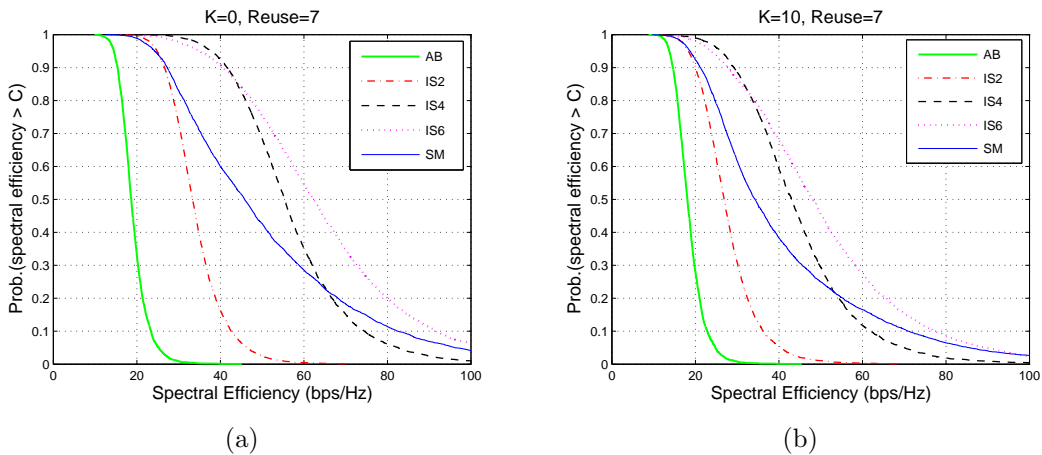


**Figure 6.15:** CCDF of the capacity when cochannel base stations transmit only one substream for a reuse factor of 7 (a)  $K=0$  (b)  $K=10$

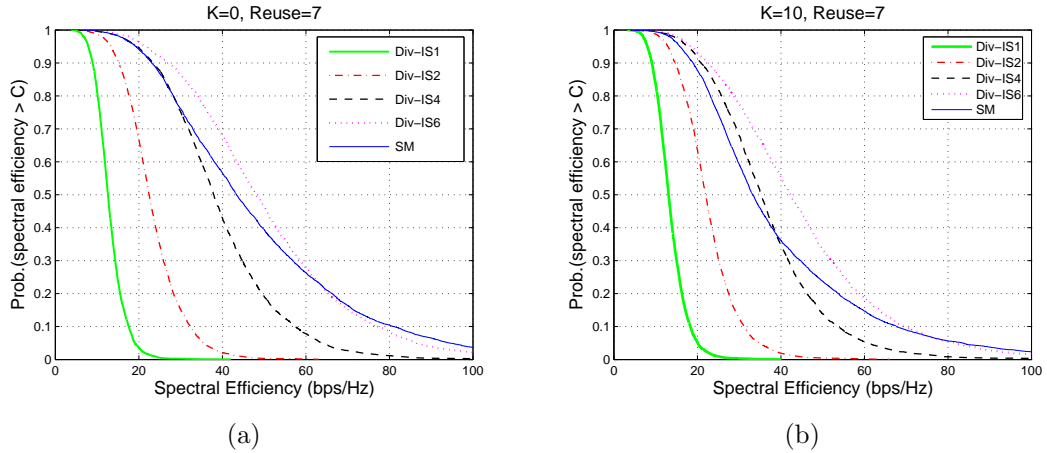


**Figure 6.16:** CCDF of the capacity with no transmitter beamforming for a reuse factor of 7 (a)  $K=0$  (b)  $K=10$

As we have done before for the  $4 \times 4$  systems, we also reduce the number of independent substreams from the cochannel base stations from 8 to 1. Results are shown in Figure 6.15. These results show the substantial performance benefit possible with the Hybrid IS6 system. For instance, the Hybrid IS6 system is better than the SM system almost everywhere in a cell. Also, for the Hybrid IS6 system, 57 bps/Hz can be achieved by 60% of the users in a cell, but only 40 bps/Hz with SM mode.

We also considered the system performance when transmit beamforming is not employed. Simulation results are shown in Figure 6.16. Comparing the results between Figure 6.11 (Tx beamforming) and 6.16 (No Tx beamforming), we notice that the degradation caused by the absence of channel state information is very small. Thus, even if we have a minor performance degradation, the benefit of not needing feedback would be substantial.

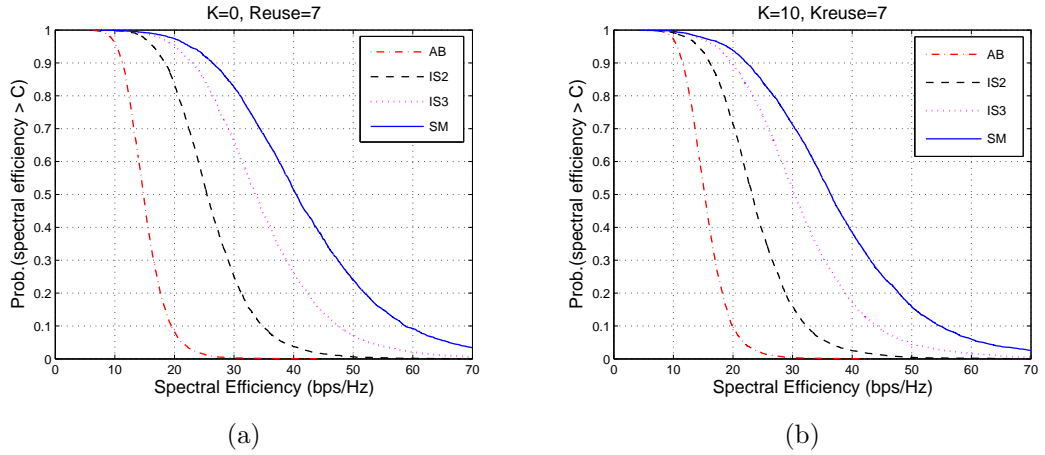


**Figure 6.17:** CCDF of the capacity for a 4x8 system for a reuse factor of 7 (a) K=0 (b) K=10

## 6.9 Capacity Distribution for a 4x8 System

Here, we adopt more antennas at the receiver than the transmitter, specifically, we assume 4 transmit and 8 receive antennas. In this case, the receiver has more ability to suppress the interference-plus-noise level. Thus, we can expect intuitively that the cases of 3 or 4 substreams are improved more than the others since, with 8 receive antennas, we can suppress the interference significantly. Figure 6.17 provides the results for a reuse factor of 7 and Ricean K factor=0 and 10. In this case, the SM system is always better than the other systems. This is true even for a K factor as large as 50, as shown in Figure 6.18.

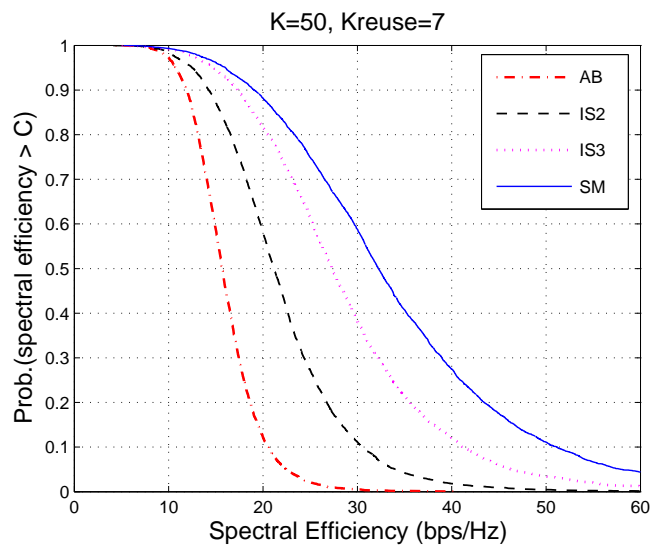


**Figure 6.18:** CCDF of the capacity for a 4x8 system for a reuse factor of 7 and  $K=50$

## Chapter 7

### CONCLUSIONS AND FUTURE WORK

In this thesis, we introduced and evaluated the performance of a hybrid MIMO system that combines spatial multiplexing and adaptive beamforming. By combining these two different multiple antenna techniques, we obtain a system that possesses properties of each. In particular, we considered the case of 4 transmit and 4 receive antennas in a multi-cell environment. We permitted from 1 (adaptive beamforming) to 4 (spatial multiplexing) independent substreams to be transmitted, and we evaluated the resulting capacity.

Although the SM mode is surprisingly robust (as found in [15]), the hybrid systems can provide improved performance in a multi-cell environment. Through simulations, we showed that the hybrid systems achieve higher efficiencies for users who are farther from the base station or, alternatively, provide higher capacities to a larger percentage of the cell. These conclusions apply over a wide range of target outage probabilities and Ricean K factors.

We also performed simulations for other numbers of antennas and antenna configurations, specifically 8 transmit and 8 receive antennas and 4 transmit and 8 receive antennas. For the 8x8 antenna system, hybrid systems show more improvement,

in terms of capacity, relative to the SM mode. However, when the 4x8 system is considered, the SM mode is better than a hybrid system because of the fact that the receiver has more ability to suppress interference.

As another hybrid system, the combination of simple diversity (no transmit beamforming) and SM was considered. The simple diversity system evaluated in this thesis is the special case of an AB system when the transmit beamforming vector is just a unit vector. Surprisingly, this system shows comparable performance to that for the hybrid of SM and AB. The implication is that feedback channel information can be avoided with little loss.

Some challenges for the future include developing realistic algorithms for implementing these hybrid systems and possibly developing a method for adaptation within a cell to use the most advantageous mode for that part of the cell. Another future effort could be the joint optimization of the transmit beamforming since, in this thesis, transmit beamforming vectors are independently optimized which does not necessarily lead to optimum performance.

## REFERENCES

- [1] J. H. Winters. Optimum combining in digital mobile radio with cochannel interference. *IEEE J. Sel. Areas in Commun.*, vol. SAC-2, no. 4, pp. 528-539, July 1984.
- [2] S. Alamouti. A simple transmit diversity technique for wireless communications. *IEEE J. Sel. Areas in Commun.*, vol. 16, no. 8, pp. 1451-1458, Oct. 1998.
- [3] H. Sampath, S. Talwar, J. Tellado, V. Erceg, and A. Paulraj. A fourth-generation MIMO-OFDM broadband wireless system: design, performance, and field trial results. *IEEE Commun. Mag.*, vol. 40, no. 9, pp. 143-149. Sept. 2002.
- [4] R. D. Murch and K. B. Letaief. Antenna systems for broadband wireless access. *IEEE Commun. Mag.*, vol. 40, no. 4, pp. 76-83. April 2002.
- [5] B. Friedlander and S. Scherzer. Beamforming versus transmit diversity in the downlink of a cellular communication system. *IEEE Trans. on Veh. Technol.*, vol. 53, no. 4, pp. 1023-1034, July 2004.

- [6] G. J. Foschini and M. J. Gans. On limits of wireless communications in a fading environment when using multiple antennas. *Wireless Pers. Commun.*, vol. 6, no. 3, pp. 311-335, 1998.
- [7] I. E. Telatar. Capacity of multiantenna Gaussian channels. *Eur. Trans. Telecommun.*, vol. 10, no. 6, pp. 585-595, Nov. 1999.
- [8] D. Gesbert, M. Shafi, D. Shiu, P. J. Smith, and A. Naguib. From theory to practice: An overview of MIMO space-time coded wireless systems. *IEEE J. Sel. Areas in Commun.*, vol. 21, no. 3, pp. 281-302, April 2003.
- [9] S. Catreux, P. F. Driessen, and L. J. Greenstein. Data throughputs using multiple-input multiple-output (MIMO) techniques in a noise-limited cellular environment. *IEEE Trans. on Wireless Commun.*, vol. 1, no. 2, pp. 226-235, April 2002.
- [10] S. Catreux, L. J. Greenstein, and V. Erceg, Some results and insights on the performance gains of MIMO systems. *IEEE J. Sel. Areas in Commun.*, vol. 21, no. 5, pp. 839-847, June 2003.
- [11] R. S. Blum. MIMO capacity with interference. *IEEE J. Sel. Areas in Commun.*, vol. 21, no. 5, pp. 793-801, June 2003.
- [12] R. S. Blum, J. H. Winters, and N. R. Sollenberger. On the capacity of cellular systems with MIMO. *IEEE Commun. Letts.*, vol. 6, no. 6, pp. 242-244, June 2002.

- [13] S. Catreux, P. F. Driessen, and L. J. Greenstein. Simulation results for an interference-limited multiple-input multiple-output cellular system. *IEEE Commun. Letts.*, vol. 4, no. 11, pp. 334-336, November 2000.
- [14] S. Catreux, P. F. Driessen, and L. J. Greenstein. Attainable throughput of an interference-limited multiple-input multiple-output cellular system. *IEEE Trans. on Commun.*, vol. 49, no. 8, pp. 1307-1311, August 2001.
- [15] F. R. Farrokhi, A. Lozano, G. J. Foschini, and R. A. Valenzuela. Spectral efficiency of FDMA/TDMA wireless systems with transmit and receive antenna arrays. *IEEE Trans. on Wireless Commun.*, vol. 1, no. 4, pp. 591-599, Oct. 2002.
- [16] W. C. Jakes Jr., *Microwave Mobile Communications* 2nd edition. Wiley, New York, 1994.
- [17] T. Rappaport. *Wireless Communications*. Prentice-Hall, Upper Saddle River, New Jersey, 1995.
- [18] M. D. Yacoub. *Foundations of Mobile Radio Engineering*. CRC Press, New York, 1993.
- [19] P. F. Driessen, and G. J. Foschini. On the capacity formula for multiple-input multiple-output channels: A geometric interpretation. *IEEE Trans. on Commun.*, vol. 47, no. 2, pp. 173-176, Feb. 1999.

- [20] J. G. Proakis. *Digital Communications* 4th edition. McGraw-Hill, 2001.
- [21] J. H. Winters. Smart antennas for wireless systems. *IEEE Pers. Commun.*, vol. 5, no. 1, pp. 23-27, Feb. 1998.
- [22] K. Sheikh, D. Gesbert, D. Gore, and A. Paulraj. Smart antennas for broadband wireless access networks. *IEEE Commun. Mag.*, vol. 37, no. 11, pp. 100-105, Nov. 1999.
- [23] M. Chryssonmallis. Smart antennas. *IEEE Ant. and Prop. Mag.*, vol. 42, pp. 129-136, July 2000.
- [24] T. M. Cover, and J. A. Thomas. *Elements of Information Theory*. Wiley, New York, 1991.
- [25] S. Haykin. *Adaptive Filter Theory*. Prentice Hall, Upper Saddle River, New Jersey, 2002.
- [26] J. Litva and T. Lo. *Digital Beamforming in Wireless Communications*. Artech House, Massachusetts, 1996.
- [27] G. J. Foschini, G. D. Golden, and R. A. Valenzuela. Simplified processing for high spectral efficiency wireless communication employing multi-element arrays. *IEEE J. Sel. Areas in Commun.*, vol. 17, no. 11, pp. 1841-1852, Nov. 1999.

- [28] G. D. Golden, G. J. Foschini, R. A. Valenzuela, and P. W. Wolniansky. Detection algorithm and initial laboratory results using V-BLAST space-time communication architecture. *Electron. Lett.*, vol. 35, no. 1, pp. 14-15, Jan. 1999.